Preparation and Characterization of a Novel Porous Magnetic Chitosan-g-RMF Bead for Phenolic Compound Adsorption

Jalil Heydaripour

Submitted to the
Institute of Graduate Studies and Research
in partial fulfillment of the requirements for the degree of

Doctor of Philosophy
in
Chemistry

Eastern Mediterranean University
January 2019
Gazimağusa, North Cyprus

Approval of the Institute of Graduate Studies and Research

Assoc. Prof. Dr. Ali Hakan Ulusoy
ActingDirector

I certify that this thesis satisfies the requirements as a thesis for the degree of Doctor of Philosophy in Chemistry.

Prof. Dr. İzzet Sakalli
Chair, Department of Chemistry

We certify that we have read this thesis and that in our opinion it is fully adequate in scope and quality as a thesis for the degree of Doctor of Philosophy in Chemistry.

Assoc. Prof. Dr. Hayrettin Ozan Gulcan
Co-Supervisor

Assoc. Prof. Dr. Mustafa Gazi
Supervisor

Examining Committee

1. Prof. Dr. Okan Sirkecioğlu
2. Prof. Dr. Hayal Bülbül Sönmez
3. Prof. Dr. Elvan Yilmaz
4. Assoc. Prof. Hatice Ataçağ Erkurt
5. Assoc. Prof. Dr. Mustafa Gazi

ABSTRACT

Many industries such as pharmaceuticals, dye manufacturing, fungi and pest control, petroleum refineries etc. generate a huge amount of effluents containing phenolic compounds. These Phenolic compounds have been known to exhibit toxic effects on both humans and aquatic biota. Also, consumption of potable water containing these phenolic compounds can have undesired effects on human health since they are suspected to be carcinogenic and can cause liver damage even at very low concentrations. Hence, it is essential to properly treat industrial waste containing phenols before discharge into the environment.

In this study, we proposed a simple hydrothermal method to synthesize a magnetic mesoporous resin (m-RMF) and magnetic porous resin grafted onto chitosan beads (R-g-Ch) and applied it for removal of two phenolic compounds (4- Chloro phenol and phenol) via adsorption.

The as-synthesized adsorbents; m-RMF and R-g-Ch were characterized using Fourier Transfer Infrared (FT-IR), scanning electronic microscopy (SEM), vibrating sample magnetometer (VSM), X-ray diffraction (XRD), thermogravimetric (TG) and derivative thermogravimetric (DTG) analysis. Batch adsorption studies were conducted under varying conditions of contact time, temperature, dosage, pH etc. to optimize the experimental conditions required for the optimum removal of phenol and 4-CP. Experimental data were then analyzed using pseudo-first order, pseudo-second order and intra-particle diffusion models. In addition, two commonly used adsorption equilibrium

isotherms i.e. the Freundlich and Langmuir isotherm models were utilized to analyze the equilibrium isotherms for the adsorption of both phenolic compounds.

The collected results indicate that the adsorption process fitted the Langmuir isotherm model well in both cases which implies monolayer adsorption. The maximum adsorption capacity of R-g-Ch was found to be 180.9 mg/g and 95.5 mg/g for phenol and 4-CP while that of m-RMF was 2.49 and 1.5 mmol/g respectively. Equilibrium uptake of both phenols increased with an increase in initial concentration while the adsorption was found to be highly pH dependent with maximum removal obtained in the alkaline pH. The kinetics of the adsorption process was well explained by the pseudo-second-order kinetic model. Thermodynamic parameters (Gibbs free energy $\Delta G°$ at 298K, -14.37 and -14.29 kJ mol^{-1}, enthalpy $\Delta H°$, -23.29 and -15.54 kJ mol^{-1}, and entropy $\Delta S°$, -29.9 and -4.2 J mol^{-1} K^{-1} for phenol and 4-chlorophenol respectively) were also calculated. The overall adsorption process was irreversible, spontaneous, exothermic and feasible within the range of 298.15–318K.

These results suggest that both the R-g-Ch porous beads and m-RMF could be used as efficient adsorbents for remediation of waste water containing phenols and 4-CP.

Keywords: Phenol, 4-Chlorophenol, Chitosan, Melamine, Resorcinol

ÖZ

Farmasötikler, boya imalatı, mantarlar ve haşere kontrolü, petrol rafinerileri vs. gibi pek çok endüstri, fenolik bileşikler içeren çok miktarda atık su üretir. Bu Fenolik bileşiklerin, hem insanlar hem de suda yaşayan biyota üzerinde toksik etkiler gösterdiği bilinmektedir. Ayrıca, bu fenolik bileşikleri içeren içilebilir su tüketiminin kanserojen olduğundan şüphelenildiğinden ve çok düşük konsantrasyonlarda bile karaciğer hasarına neden olabileceğinden insan sağlığı üzerinde istenmeyen etkileri olabilir. Bu nedenle, çevreye boşalmadan önce fenol içeren endüstriyel atıkların uygun şekilde arıtılması esastır.

Bu çalışmada, kitosan taneciklerine (Rg-Ch) aşılanmış manyetik bir gözenekli reçine (m-RMF) ve manyetik gözenekli reçinenin sentezlenmesi için basit bir hidrotermal yöntem önerdik ve iki fenolik bileşiğin (4-Kloro fenol ve fenolün) adsorpsiyon yoluyla arıtılması için uygulama yapıldı.

Sentezlenmiş adsorbanlar; m-RMF ve Rg-Ch, Fourier Transfer Infrared (FT-IR), taramalı elektronik mikroskopi (SEM), titreşimli örnek manyetometre (VSM), X ışını kırınımı (XRD), termogravimetrik (TG) ve türev termogravimetrik analizi (DTG) kullanılarak karakterize edildi. Fenol ve 4-CP'nin optimum şekilde arıtılması için gereken deneysel koşulları optimize etmek için çeşitli temas süresi, sıcaklık, dozaj, pH vb. Koşullar altında adsorpsiyon çalışmaları seri olarak yapılmıştır. Deneysel veriler daha sonara pseudo birinci dereceden, pseudo ikinci dereceden ve parçacık içi difüzyon modelleri kullanılarak analiz edildi. Ek olarak, yaygın olarak kullanılan iki adsorpsiyon denge izotermi, diğer

bir deyişle Freundlich ve Langmuir izoterm modelleri, her iki fenolik bileşiğin adsorpsiyonu için denge izotermlerini analiz etmek için kullanılmıştır.

Toplanan sonuçlar, adsorpsiyon işleminin Langmuir izoterm modelini her iki durumda da tek tabakalı adsorpsiyonla uyumlu olduğunu göstermektedir. R-g-Ch'nin maksimum adsorpsiyon kapasitesi fenol ve 4-CP için 180.9 mg / g ve 95.5 mg / g iken m-RMF'nin sırasıyla 2.49 ve 1.5 mmol / g olduğu bulundu. iki fenolün denge alımı, ilk konsantrasyondaki artışla artarken, adsorpsiyonun, alkalin pH'ta elde edilen maksimum arıtmaya bağlı olarak yüksek pH'a bağlı olduğu bulundu. Adsorpsiyon işleminin kinetiği sözde (pseudo) ikinci dereceden kinetik model ile iyi açıklanmıştır. ermodinamik parametreler (Gibbs serbest enerjisi ΔG°, 298K, -14.37 ve -14.29 kJ mol-1, entalpi ΔH°, -23.29 ve -15.54 kJ mol^{-1} ve entropi S°, -29.9 ve -4.2 J mol Ayrıca fenol için -1 K^{-1} ve sırasıyla 4-klorofenol) hesaplandı. Genel adsorpsiyon işlemi, geri dönüşümsüz, kendiliğinden, ekzotermik ve 298.15-318°K aralığında uygulanabilirdi.

Bu sonuçlar, hem R-g-Ch gözenekli taneciklerinin hem de m-RMF'nin, fenoller ve 4-CP içeren atık suyun iyileştirilmesi için etkili adsorbanlar olarak kullanılabileceğini göstermektedir.

Anahtar Kelimeler: Fenol, 4-Klorofenol, Kitosan, Melamin, Rezorsol

ACKNOWLEDGMENT

It gives me immense pleasure to express my heartfelt gratitude and thanks to my wonderful parents, Mr. Safarali Heydaripour and Mrs. Kobra Heydari, my sisters and my brothers. Without their blessings I would not have come into this world nor had this excellent opportunity of doing my Ph.D. study on this topic.

Foremost, I would like to express my sincere gratitude to my advisor Assoc. Prof. Dr. Mustafa Gazi for his continuous support during my Ph.D. study and research. His patience, motivation, enthusiasm, and immense knowledge about my topic guided me constantly while I was doing my research and writing this thesis. I could not have imagined having a better advisor and mentor.

I am also hugely appreciative of Assoc. Prof. Dr. Hayrettin Ozan Gülcan, especially for sharing his expertise on the synthesis of medicinal organic compounds so willingly, and for being so dedicated to his role as my co-supervisor.

Besides my supervisor and co-supervisor, I would like to thank the rest of my thesis committee: Prof. Dr. Okan Sirkecioğlu, Prof.Dr. Hayal Bülbül Sönmez, Prof. Dr. Elvan Yilmaz, and Assoc. Prof. Dr. Hatice Ataçağ Erkurt, for their encouragement, insightful comments, and hard questions.

I also want to appreciate the assistance rendered by Prof. Dr. Osman Yilmaz, which included but was not limited to his valuable suggestions and constant support.

Finally, I wish to put on record my deep sense of gratitude and regards to the Pharmacy Faculty members, Prof. Dr. Mustafa Fethi Şahin, Prof. Dr. Gönül Şahin, Prof. Dr. Müberra Koşar, Assoc. Prof. Dr. Emre Hamurtekin, Assoc. Prof. Dr. Hayrettin Ozan Gülcan, Assist. Prof. Dr. Aybike Yektaoğlu, Assist. Prof. Dr. Emine Vildan Burgaz, Assist. Prof. Dr. Hasip Cem Özyurt Assist. Prof. Dr. İmge Kunter, Assist. Prof. Dr. Jale Yüzügülen, Assist. Prof. Dr. Mehmet İlktaç, Assist. Prof. Dr. Tuğba Erçetin , Dr. Metin Çelik, Sr. Instr. Canan Gülcan, Sr. Instr. Emine Dilek Özyilmaz, Sr. Instr. Leyla Beba Pojarani. Sr. Instr. Mustafa Akpinar, Emine Alpsoy Ertoprak, Mehmet Kurmal, Şima kubilay and Osmanvesal, for their able support and encouragement all through my Ph.D. studies and research work. I am eternally grateful to you all.

TABLE OF CONTENTS

LIST OF TABLES

LIST OF FIGURES

LIST OF SCHEMES

Chapter 1

INTRODUCTION

1.1 Environmental pollution

Environmental pollution is an undesirable change we are facing in our environment today. Pollution is simply the introduction of contaminants/pollutants into the natural environment that causes harm to the environment, human health and other living organisms, or damages the ecological system as a whole. When the concentration of any substance in the environment is more than the permissible level, it is considered a pollutant. Studies have shown that environmental water pollution is mainly related to human activities which include unsupervised discharge of domestic, industrial and agricultural wastes into water bodies, application of pesticides by farmers, leaks of radioactive materials, gas emissions into the atmosphere etc. [1].

For decades, water was considered to be pure and uncontaminated if it was odorless, colorless and tasteless. However, no water is regarded as completely pure because it contains certain amount of suspended and dissolved solids, minerals, gases as well as biological life. At present times, all concepts related to water contamination has been modified. It simply means that clear, odorless and tasteless water may possess undesirable substances such as radioactive nuclides, toxic metals, organic contaminants, and emerging contaminants which when present in limits beyond the acceptable range are harmful to both humans and the aquatic habitat at large [2].

Water is required by all living things for their survival and existence on the planet. As one of the most important commodities which man has exploited in the world today it has a high tendency to get polluted easily. Rising global population and limited/diminishing quantity of utilizable water on the earth has led to concerns that the world might experience a scarcity of fresh water in the coming years. In line with this, concerted efforts are now focused on the need to preserve and improve water quality at all times.

1.2 Water Pollution and water pollutants

Water Pollution is a result of the discharge of undesirable substances either directly or indirectly into water bodies. For example, water contamination occurs when chemical and mineral fertilizers from farms or factories flow into the rivers, oceans and underground waters untreated. This directly affects plants and living organisms within these waters. As earlier noted, no water is regarded as completely pure however water becomes polluted when the presence of these contaminants cause unwanted alteration in the physicochemical or biological properties of water that can have undesirable results on human activity, health and survival of other living organisms.

Water pollutants are chemical, physical or biological factors that have detrimental or aesthetically unpleasing effects on aquatic life and on those that consume the water. They can be categorized as organic, inorganic and biological pollutants. Majority of these water pollutants are in form of chemicals that are suspended or dissolved in water bodies. In general, any factor can be characterized as a pollutant under certain conditions if it is present in excessive amounts that can have an adverse effect on the aquatic habitat [1].

Generally, two main sources of water contaminants have been identified and they are classified as either direct/point and indirect/non- point sources of water pollution [3]. To further clarify this, sources of water pollution that include harmful substances discharged directly from factories, wastewater treatment facilities, septic systems are termed as direct or point sources. Indirect or non-point contamination sources on the other hand are a product of soils/groundwater systems (from excess fertilizers, herbicides etc. used in agricultural lands i.e. human agricultural practices), from atmospheric gaseous emissions by automobiles, factories etc. which are also derived from human practices that are then carried into a stream by rain or water run-off. Majority of the contaminants in streams and lake are from indirect sources which in most cases tend to be much more difficult to control [4].

In broader terms, industrial, municipal and agricultural activities are the main sources of water contamination. The wastewater from homes and commercial establishments produce Municipal water pollution. Characteristics i.e. type and concentration of pollutants present in industrial wastewaters usually depends on the industry and the waste cleaning/disposal method applied in industry [5]. Also, studies have shown that there is a relationship between industrial activities, chemicals potentially disposed of and present, and their impacts on surrounding water bodies, such as biochemical oxygen demand (BOD), chemical oxygen demand (COD) and the number of suspended solids present in them. The most common pollutants in water are heavy metals, toxic organic substances like pesticides, phenols, insecticides etc., and biological microorganisms such as bacteria, fungi, pathogens which are usually referred to as biopollutants [6]. Persistent organic pollutants (POPs) are organic compounds that are resistant to environmental and synergetic characteristics of the

ecosystem and can affect human well-being, health and general body function, food production etc. [7].

Table 1.1 shows some important water contaminants and their adverse effects on both humans and the aquatic habitat. These contaminants can either be completely soluble in water, exist as particulate matter or a cumulative of both.

Table 1: Important contaminants in wastewater (Source adapted from Metcalf and Eddy, 1991)

Contaminants	Reason(s) for importance
Sediments and suspended solids (SS)	They can cover gravel beds and cause fish can find the food hardly and, also damage gill structures oh insects and fish directly. Organic sediments causing a reduction in oxygen and creating anaerobic conditions like unpleasant odors.
Biodegradable organics	The oxygen demanding nature of biodegradable organics is very important for natural water system due to secondary action of microorganism.
Pathogens and microbial contaminants	Infectious disease can be spread by contaminated water
Organic compound like phenolic compounds and inorganic compounds such as calcium, sodium and sulfate.	They are human highly toxic, carcinogenic, or mutagenic.
Refractory organics	Some refractory organics are toxic to aquatic life such as surfactants, phenols and agricultural pesticides which are more resistant to microbial degradation
Heavy metals	Usually they are in present in industrial waste water. They can enter into the food chain and can prove toxic even in the low metal concentration.
Inorganic compounds such as calcium, sodium and sulfate which is dissolved in water.	These compound are initially added to domestic water supplies, however in excessive amounts have negative effect therefore they must to be removed.
Nutrients	Discharge of these substances into water leads to increase in phosphorus and nitrogen concentration. Hence, algae and aquatic macrophytes grow in drinking water.

Table 1: Important contaminants in wastewater (Source adapted from Metcalf and Eddy, 1991)

Contaminants	Reason(s) for importance
High temperature	Increase the rate of decomposition of organic substances and causes changes in oxygen levels in the water. Therefore it may change the composition of species present in drinking water.
Emerging contaminants such as pharmaceuticals Products	They can be harmful to human health even in the low amount due to their adverse health effects.

In recent years, the effect of water pollution on human health and the aquatic biota has been a cause of rising concern. Heavy metals, dyes and phenolic compounds have been increasingly found in water in varying concentrations, sometimes beyond the permissible level. The fact that these pollutants are toxic, contaminate the aquatic environment and can be passed right up to humans in the food chain has led to the dedication of many research institutes to find concerted efforts towards reducing water pollution in the world today [8, 9].

Phenols generally are considered to be one of the most dangerous organic pollutants discharged into the environment, even more so that low concentrations of Phenolic compounds present in water can prove dangerous to living organisms. Furthermore, phenols and some of its related compounds are suspected to be carcinogenic in nature and can be toxic to both humans and aquatic life, therefore they is a need to treat waste water containing phenols before release into receiving water bodies.

With respect to increasing effluent discharge standards to the permissible level before release into the environment, many industries take into consideration different factors before selecting the most appropriate methods of treatment based on the nature of their

activities. This procedure takes into consideration the advantages and disadvantages of chemical, biological and physical treatment processes [10].

Major industrial sources of phenolic compounds are; coke oven plants, petrochemical and pharmaceutical industries, coal gas, petroleum refineries, steel mills, paints, plywood industries, synthetic resins, and plywood industries. The reported average phenolic concentrations for some of the industrial wastewaters generated by these industries are given in Table1.2.

Table 2: Industrial source and concentration of phenol

Industries	Concentration, (mg/L)
Coking plant weak ammonia liquor	580.100.000
Without diphenolization weak ammonia liquor	4-332
After diphenolization wash oil still waste	30-50
Oil refineries sour water	50-185
General wastewater	10-100
APF Separator effluent	0.3-6.8
Petrochemical benzene refinery	210
Tar distillation	300
Nitrogen works	250
Organic manufacturing	100-150
Plastic factory	200-00
Phenolic resin production	1600
Fiberboard factory	150
Fiberglass manufacturing	40-400
Aircraft maintenance	200-400

As seen from the Table above, the highest concentration of phenols (>5000 mg/L) is obtained from coke processing plants. The resin plants also produce a considerable amount of phenolic compounds with a concentration of 1600 mg/L. Phenol production in the United States ranks in the top 50 with respect to production volume for chemicals [14].

The Environmental Protection Agency (EPA) and World Health Organization (WHO) recognize that phenol is a toxic substance with serious health and ecological hazards and placed in the priority list of hazardous compounds [13]. Therefore, in order to prevent the potential adverse health effects of phenols on human and protect the environment, the Environmental Protection Agency (EPA) set the maximum concentration of phenol in treated effluents to be 0.1 mg/L [11]. The World Health Organization (WHO) on the other hand was more stringent and set the maximum concentration of phenol in potable water to be 0.001 mg/L [12]. The WHO also went as far as to declare the maximum concentrations of some phenolic compounds that can be acceptable in drinking water. These include; 2,4, 6-trichlorophenol (200 mg/L), pentachlorophenol (9 mg/L), 2- chlorophenol 2 (10 mg/L) and 4- dichlorophenol (40 mg/L) respectively. The Environmental Protection Agency (US-EPA) also included some substituted phenols (window range concentration is considered between 60 to 400 mg/L) known to be hazardous in the Federal Register. The permissible limit of phenolic compounds for industrial effluents before discharging into municipal sewers and surface waters was set at 1-5 mg/L [15, 16].

1.3 Technologies available for phenolic compounds removal

Wastewater treatment technologies can be classified into three principal categories: biological, chemical and physical procedures. Each one of these methods has its own advantages and drawbacks. According to literature, there are several reported procedures available to eliminate phenols from effluents. However, most of these treatment procedures for removing phenol from wastewater suffer from several drawbacks such as: high initial cost and disposal problems hence, they have not been used widely on the industrial scale. Also, removal and control of specific contaminants like phenols is a rigorous process in the treatment of wastewater. Natural wastewater

treatment systems are widely used in land-based applications. To date, not one treatment process can be used to effectively treat waste water from industries because of the sophisticated nature of industrial effluents (i.e. they contain more than just one pollutant). So in reality, to achieve the desired water quality required by law in the most economical way, most industries try several different combinations of treatment processes. This adds to the economic cost of production as well so most scientists are looking for inexpensive and suitable technologies to get this done.

A comprehensive literature review carried out during this research work demonstrates that research has been and still continues to combine both biological technologies and adsorption as a means of treatment to enhance the biodegradation of phenols and minimize the sludge production.

As previously mentioned, wastewater treatment procedures are divided into physical, chemical and biological processes. Examples of waste water treatment operating units and processes are displayed below [14]:

a) Physical unit operations

1. Screening
2. Comminution
3. Flow equalization
4. Sedimentation
5. Flotation
6. Granular-medium filtration

b) Chemical unit operations

1. Chemical precipitation
2. Adsorption
3. Disinfection
4. Dechlorination
5. Other chemical applications

c) Biological unit operations

1. Activated sludge process
2. Aerated lagoon

3. Trickling filters
4. Rotating biological contactors
5. Pond stabilization
6. Anaerobic digestion
7. Biological nutrient removal

These methods listed above can be used for removing phenolic compounds from wastewaters [14]. However, they are very expensive, low-efficient processes that generate toxic by-product [17]. Adsorption technique on the other hand is now widely used to remove toxic substances due to the availability and affordability of many adsorbents. The adsorption process is now regarded as the best technique for removal of phenolic compounds because it is a simple method and easy to operate [20]. For a material to serve as a suitable adsorbent, it must have the ability to concentrate specific substance(s) from solution onto its surface and retain it.

Many conventional and non-conventional adsorbents have been applied in recent times for the removal of several pollutants from wastewater. In the past few years, it is interesting to note that various biomasses and agricultural wastes have attracted attention and been used as biosorbents because they are eco-friendly and are cost-effective in nature. This process is termed as biosorption i.e. the use of biomass for separation of pollutants from an aquatic environment [21].

An important factor to consider when using nonconventional materials as adsorbents in wastewater treatment is the adsorption capacity of the adsorbent [15]. Different non-conventional adsorbents like sawdust, activated coconut shell powder, bagasse pith, rice husk ash, fly ash, peat, controlled burnt wood charcoal, wood, jute fibers etc. have been used by numerous investigators [18].

The use of polymer resins for removing phenolic compounds from wastewater have also been investigated as an effective method due to its high adsorption capacity large surface area, high purity, microporous nature, and ease of availableness [19].

1.4 Adsorption of phenol and its derivatives

From the literature survey shown in table 1.3, a wide range of adsorbents have been evaluated for the removal of phenolic compounds via adsorption. The table shows that many low-cost natural products such as wheat husk [22], jute stick [23], tobacco residues [24] and tamarind nutshell [25] have been used for phenol removal.

Table 3. Adsorbents and their performance for wastewater treatment

Adsorbent	Selectivity	Operation Condition	Adsorption/Removal	Ref.
Conventional (A) Ion exchangers Conventional				
Dowcx 50 W- X8	Phenol, p- cresol	Column	—	45
Amberlite- XAD	Phenol, p-nitro phenol, m-nitro phenol	—	—	46-48
Polymeric adsorbent	Phenols	—	—	49
Dowex 1X4	Phenol	Column	—	50
Porous polymer based on acrylic matrix	Phenol, p-nitrophenol, m-aminophenol	Batch conc: 100mg/L	60-186mg/g	51
Macroreticular resin	Phenols	—	—	52
Weakly basic anion Exchanger	Phenols	—	—	53
Anion exchange resin	Phenols	—	—	54-59

Table 3. Adsorbents and their performance for wastewater treatment

Adsorbent	Selectivity	Operation Condition	Adsorption/Removal	Ref.
Chelating Ion exchange in iron (III) form	Chlorophenols, nitrophenols	Column Conc:100mg/L	28-100 precent	62
(B) Inorganic				
Zinc silicate in iron (III) form	Pyrogallol, Catechol, O-Cresol, Phenol	Column Conc:1mg/mL, equil	36-133mg/g	34
tannic molybdate	Phenols	Column	—	63
Zinc silicate	m-,p- cresol, 4-chlorophenol, O-Cresol	Impregnated paper	—	64
Stannic tungstate	Phenols	TLC	—	65
Ion- exchange resins	Phenol	—	—	66-67
Iron (III) diethanol amine	Phenol, resorcinol, o-chlorophenol,	Column Conc:1mg/mL	3-29mg/g	69
Hydrous ZnS	Substituted Phenols	Batch	—	70

Table 3. Adsorbents and their performance for wastewater treatment

Adsorbent	Selectivity	Operation Condition	Adsorption/Removal	Ref.
Iron (III) hexamine	Resorcinol,quinol, phlorog-lucinol,	Column, impregnated	21-92mg/g	72
Iron (III) morpholine	Phenol, m-aminophenol,α-naphtol	Column Conc:1mg/mL	24.8-118.9mg/g	73
Am on-conventional Activated				
Activated carbon from straw and used rubber	Phenol, p-chlorophenol	Batch, conc:6.03 mmol/L, equil time:2h	2.08 mmol/g	21
Activated carbon from apricot stone shellActivated carbon matrix	2,4- Dinitro- and 2.4- di-chlorophenols	Batch, conc:10 mg/L,	36-65%	29
Activated carbon matrix	Phenols and substituted phenols	Batch	—	38,41,74-94
Burn wood charcoal	Phenols	Batch, conc:25- 400	1-7 mg/g	39
Activated carbon from agricultureal raw material and Spanish	Chlorophenols	—	—	93
An Activated carbon from fertilizer waste slurry	4- Nitrophenol. 2,4,6-trinitrophenol,4-chlorophenol, resorcinol	Batch	—	94

Table 3. Adsorbents and their performance for wastewater treatment

Adsorbent	Selectivity	Operation Condition	Adsorption/Removal	Ref.
Activated carbon from jute fiber	Phenol	Batch, conc:100 mg/L, equil time:5h	28.5 mg/g, 77.9 percent	95
Granual activated carbon	Phenol	—	—	96-101
Biologiocal activated carbon	Phenol, 2,4- Dichlorophenol	Batch, conc:100 and 116 mg/L, pH 7, equil	25.04and 43.75 mg/g	102
Surface modified carbon block	Phenols	—	—	103
Surface treated acivated carbon	Phenol	Column	—	104
Impregnated fly ash	Phenols, o- and m- cresols, o- and m- nitrophenol	Batch conc: 100mg/L	9- 46 percent	30
Montmorillonite based sorbent	Phenols, 2,4,5- trichlorophenol,	Batch	—	31
Chemically treated saw dust	Pyrogallo, pyrocatechol	Batch, conc:100mg/L, pH 6	28-52 mg/g	33
Peat, fly ash and bentonite	Phenol	Batch, conc:1mg/L, pH 4-5, equil time:5 and 16h	42.4 percent	35

Table 3. Adsorbents and their performance for wastewater treatment

Adsorbent	Selectivity	Operation Condition	Adsorption/Removal	Ref.
-Activated carbons from used tea leaves	Phenol, o-, m- cresol, 4-chlorophenol	Batch, Column, con:500 mg/g	80.2- 438.4 mg/g	37
Organobentonite	Phenol, m- chlorophenol	Batch, conc:100mg/L, equil time:12h	80 percent	105
Organo clays	P- chlorophenol, tannic acid	—	—	106,107
Soil	Sustituted phrnols	—	—	108,109
Dolamite	Phenols	—	—	110
Sediment fractions	Phenols	—	—	111
Silt stone	Phenols	—	—	112
Aquifer material and natural sediments	Pyrnated phenols	—	—	113
Na and K -montmorillonite	Phenol, m- cresol, m-nitrophenol, p- boromophenol	Batch, pH 5.4-6.5, equil time:24h	29.48-109.4 mg/g	114
Dual cation	Phenol, p- nitrophenol	Batch, equil time:2h	3.4-34.4mg/g	115

Table 3. Adsorbents and their performance for wastewater treatment

Adsorbent	Selectivity	Operation Condition	Adsorption/Removal	Ref.
Modified bentonites	Phenols	—	—	116
Lake sediments	Phenols	Batch, pH 7, equil time:40h	28-67mg/g	117
Bagasse fly ash	2,4-Trinitrophenol	Batch	—	118
Activated sluge	Phenols	—	—	120
Hexadecyl trimethylammonium	Pentachlorophenol	Batch	—	121
Coal, fly ash and activated carbon	Phenol	Batch	—	122
Fly ash	Phenol	Batch	91, 27.9mg/g	123-129
Actuvated sludge ans fly ash	Phenol	Batch	—	130
Biopolymers	Phenol	Batch	—	131
Puled wood fiber	2,4- Dichlorophenol, 2,4,5-trichlorophenol	—	—	132

Table 3. Adsorbents and their performance for wastewater treatment

Adsorbent	Selectivity	Operation Condition	Adsorption/Removal	Ref.
Polyurethane foams	Phenols	Batch	—	133
Fertilizer waste slurry	2,4 Dinitrophenol	—	—	134
Low coast carboneous adsorbent	2,4,6 Trinitrophebol, 4-nitrophenol, 4- chlorophenol,	Batch	—	135
Activated carbone from bamboo	Phenol	Batch	—	136
Marine sediments	2,4-Dicholorophenol	Batch, conc:5-20 mg/L	1.5-4 mg/g	137
Bacillus subtilis	2,4-6, Tricholorophenol	Batch	—	138

Chapter 2

PROPERTIES, CHARACTERIZATION AREAS OF APPLIED CHEMICALS

2.1 Chitosan and characterization

Chitosan is a natural polyamine saccharide which is derived from the deacetylation of chitin, which contains a predominated unbranched polysaccharide ((1→4)-2-acetamido-2-deoxy-d-glucose). Chitin on its own is extracted from many sources such as crabs, fungi, prawns, insects and other crustaceans [139]. The unique properties of chitosan such as its biocompatibility, hydrophilicity, non-toxicity, biodegradability, and adsorption properties have made it an adequate polymer for many applications including enzyme immobilization application, drug delivery etc.[140].

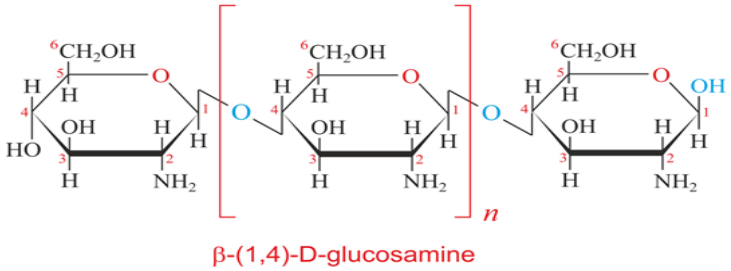

Scheme 1: Structure of chitosan

As it is clearly understood, the simplicity of chemical modification is one of the great advantages of the chitosan structure. Chemical modifications of chitosan provide new derivatives that exhibit different or improved properties when compared to chitosan itself such as high adsorption capacity, superior biological activities and

physiochemical properties coupled with high resistance to dissolve in extreme media/ conditions. Chitosan derivatization can be achieved by grafting (inserting functional groups) or cross-linking reactions (linking the macromolecular chains to each other). Grafting of chitosan with extra functional groups increases the number of active sites present on the chitosan backbone leading to an observable increase in the adsorption capacity of chitosan. Unlike the grafting process, the adsorption capacity slightly decreases with cross-linking reactions due to the binding of the amine and hydroxyl groups with the chemical cross-linker which in turn prevents it from adsorbing the contaminants [141].

2.2 Melamine

1, 3, 5-triazine-2, 4, 6-triamine commonly known as Melamine, has three amino groups on its chemical structure. These functional groups are used in the synthesis of melamine–formaldehyde resin polymers. Nitrogen makes up about 66 % of melamine mass; therefore it can be used as filler for protein-rich diets by unethical manufacturers [142-144].

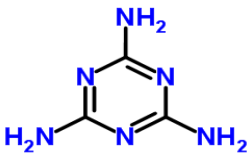

Scheme 2: Structure of Melamine

Another form of melamine is the melamine foam which has a 3D structure that is used for purifying liquids [145], to clean surfaces [146], absorb sound [147], serve as insulators from heat and electricity, in building components, aircraft insulation, packaging and sanitary ware [148]. The melamine-formaldehyde foam is rich in nitrogen and possesses high thermodynamic stability which makes it useful for fire-

retardant applications. In addition, the three-dimensional structure of the melamine-formaldehyde foam can be easily broken down to produce a fragile product so by using the chemical and physical methods, we can improve the toughness of these resins [149,150].

Modification of Melamine resin can be achieved using any of the following procedures: Firstly, the amino functionality of the melamine can be changed [151]; the second changes can occur on the hydroxyl group during synthesis by adding a modifier [152,153,154]; third, pre-condensate of the melamine resin can be synthesized by incorporating a flexible polymer or nanoparticles into it [150]. In this system, the size of polymer cell matrix plays a multifunctional role as the nucleating agent in the polymer matrix thereby reducing cell size, improving size uniformity and toughness of foam resin [155].

Apart from polymers, Fe_3O_4 nanoparticles have also been used widely by many researchers to form melamine pre-condensates [156-158]. The large number of hydroxyl methyl group present on Melamine resin may react with the carboxylate on the surface of Fe_3O_4 nanoparticles under certain conditions. Therefore the possibility of cracks will decrease in the foam due to accumulation. Moreover, the synthesis of magnetic melamine foam has a variety of applications in the electronics industry as magnetic shielding materials [159], absorbing stealth materials [161,162], microbial culture [163], biomedical research [164], scientific instrument and communication equipment etc. Another most important application of the magnetic foam is as a carrier agent to grow bacteria cells by using weak magnetic fields to stimulate the living cell. The magnetism was applied to improve cell proliferation on the microorganism, besides it is conducive for the microorganisms growth cycle and greatly improves the

biological activity of the microorganism and cells [165]. Adding metal chelating agents helps to increase the dissolution of iron oxides in the melamine structure to produce a more uniform melamine foam resin [161]. Also, Magnetic properties conferred on the melamine foams help to improve its efficiency in wastewater treatment [159,166].

Magnetic foam production could be improved due to a low-Efficiency evaluation of sewage treatment and large area conditions. They are used broadly in the foam synthesis of polystyrene [167] and polyurethane [168]. These materials produced have good mechanical properties, but there is a limitation to the usage of magnetic foams due to its low heat distortion point (particularly below 100 ^{o}C). The high flammability of this material can be controlled by adding halogen or phosphorus. Unfortunately, this can result to the formation of halogen halides which acts as contaminants. Besides, the magnetic foams have lower stability in normal weather [169].

2.3 Resorcinol−formaldehyde resin

Hydrophilic resins are a common type of adsorbents used in water treatment because they exhibit favorable interaction(s) with hydrophilic groups of some pollutants [170]. Resorcinol−formaldehyde resin has been increasingly used in metal adsorption due to the availability of abundant hydroxyls groups on its backbone. This polymer resin have excellent characteristics such as good stability, high mechanical strength, and is rich in amino groups [171, 172].

Recently, formaldehyde-resorcinol and formaldehyde-melamine resins were combined to produce a Resorcinol−formaldehyde−melamine resin (RMF) [173]. RMF resins possess abundant hydrophobic (unsaturated rings) and hydrophilic groups (such

as imino groups, hydroxyls, and ether linkages), so they can serve as good candidates as adsorbents to remove pollutants from aqueous matrices. The major disadvantage of the RMF resin is that its non-selectivity decreases [174-178].

2.4 Nanomagnetic Iron (Fe_3O_4)

Today, the interest in the study of Fe_3O_4 nanoparticles (NPs) has increased in various research fields, such as drug delivery and targeting, information storage and magnetic separation, due to their magnetic and electrochemical properties [179]. Magnetite (Fe_3O_4) has outstanding magnetic and semiconducting properties. It can act as a filler and can also be combined with polymers that are used for water purification and medical applications [180]. Magnetic polymers can create quick, efficient means to eliminate pollutants from aqueous waste streams therefore they can be applied during filtration in water treatment technology [181]. They can also be a cost efficient means to reduce the pollution of wastewaters since they can bind to the environmental pollutants and be separated magnetically. A good example is magnetic activated carbon which can be easily and rapidly separated from solutions using an external magnetic field. The different magnetic adsorbents mainly applied for removing water pollutants are based on activated carbon fibers, polymers (chitosan, cellulose, alginate etc.) ion exchange resins, solvent extractors, zeolites, composites, nanoparticles, nano bowls adsorbents [181–187].

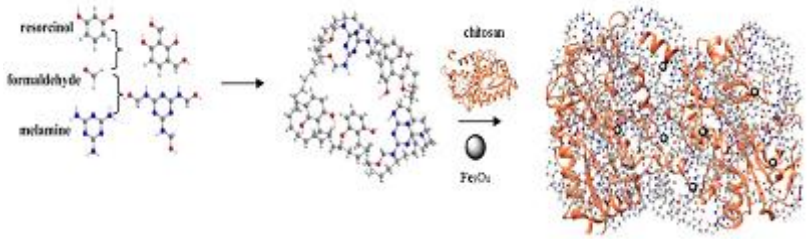

Scheme 3: Synthesis of R-g-Ch polymer

Chapter3

Materials and method

3.1 Materials

All chemicals were of analytical reagent grade and used as received without further purification. Melamine, resorcinol, formaldehyde, chitosan (MW: 50,000-190,000), epichlorohydrin, ethanol, sodium hydroxide, hydrochloric acid, $(NH_4)Fe(SO_4)_2.6H_2O$, $FeCl_3$, ammonia solution, sodium carbonate, phenol, para chlorophenol (4-CP) were purchased from Aldrich, Germany. All solutions were prepared by using deionized water.

3.2 Synthesis of materials

3.2.1 Synthesis of Fe_3O_4 nanomagnet

Magnetite (Fe_3O_4) nanoparticles were prepared by co-precipitation of $(NH_4)Fe(SO_4)_2.6H_2O$ and $FeCl_3$ (1:2 molar ratio) with ammonia solution (NH_4OH). In a typical reaction, a mixture of $FeCl_3$ (160 ml, 1 M) and $(NH_4)Fe(SO_4)_2.6H_2O$ (40 ml, 1 M) was prepared and carefully added to the boiling alkaline solution (30 ml NH_4OH; 28% w/w) under nitrogen gas in the fume cupboard with vigorous stirring. The resulting solution was then aged in the mother liquor for 90 min at 80^oC before cooling to room temperature. The black magnetite nanoparticles were isolated by magnetic decantation, purified by centrifugation (4000-6000 rpm, 20 min) and then dried at 80^oC for 12 h [189].

3.2.2 Synthesis of porous resorcinol-melamine-formaldehyde (RMF) resin

Porous RMF resin was synthesized by reacting Resorcinol (2.02 gr, 0.1mole), melamine (2.522 gr, 0.1mole), formaldehyde (21 ml, 0.3 moles) and 2M HCl (200 ml) for 5 hours at 126^{o}C in an oil bath under constant shaking. The solid resinous product formed was then separated from the solution via filtration. To remove unreacted monomers, the resulting powder formed was washed repeatedly with hot water before applying diethyl ether to eliminate the excess p- cresol-formaldehyde copolymer which might have remained during the process. Finally, the purified copolymer resin was ground into powder, sieved to achieve size uniformity and stored in a desiccator for further use.

To prepare glycidol RMF, 3 g of RMF resin previously prepared was added to epichlorohydrin (20 ml) in a 100ml two-neck round-bottom flask and heated up to 95 ^{o}C under reflux with constant stirring. Then, 5 ml ethanolic solution of sodium hydroxide (5%) was added dropwise to the mixture. After 3 hours, 200 ml of acetone was added to the reaction mixture in a 250 ml beaker and filtered by glass fiber in order to remove any salt produced during the process. To ensure the complete removal of unreacted epichlorohydrin and acetone, the residue was transferred to a rotary evaporator at 85^{o}C. Product (glycidol RMF resins) obtained was washed several times with distilled water and dried in the oven at 60^{o}C for 24 hours.

3.2.3 Synthesis of porous magnetic RMF grafted chitosan (R-g-Ch) beads

Powdered chitosan (30 mmol as glucosamine residue, 4.83 g) was dissolved in 2% w/w acetic acid (200 ml) and diluted to 250 ml with methyl alcohol. To ensure complete dissolution, the polymer solution was stirred overnight at room temperature. Glycidol RMF resin mixture (2 gr, 15mmol, and 15.5 mL) was prepared by adding 10 mL of ethanolic acid solution (HCl, 0.5 M) to the solid resin before transferring it

under constant agitation to the already prepared polymer mixture at 60^{o}C for 2 hours. The resin polymer mixture then was filtered and washed with deionized water. The resulting precipitate RMF-g-chitosan was dried in an oven at 50^{o}C.

RMF-g-chitosan (0.8 g) was dissolved in 50 mL acetic acid (2%) before adding nano-Fe_3O_4. The mixture was stirred for 1 hour at room temperature and then dropped into NaOH (1M) solution by syringe under mechanical stirring. The beads formed were left in the NaOH solution for 4 hours to stabilize, washed severally with deionized water till the pH of the filtrate was neutral (i.e. 7). To fabricate porosity, beads were freeze dried (-80^{o}C for 24 hours) before lyophilization was carried out for 72 hours. The lyophilization stage in the synthesis of the porous RMF-g-chitosan beads occurs in three stages. The first stage takes about 10 minutes under vacuum 6.4 mbar at -40^{o}C. In the second stage, the temperature is increased to -15^{o}C, vacuum pressure was set at 1.4mbar for 20 minutes while in the final stage the temperature was raised to 30^{o}C and vacuum pressure decreased to 0.98 mbar for 72 hours. On completion of the

lyophilization process, brown porous chitosan scaffold was prepared [190]. All the steps involved in the reaction pathway are shown in scheme 4 below.

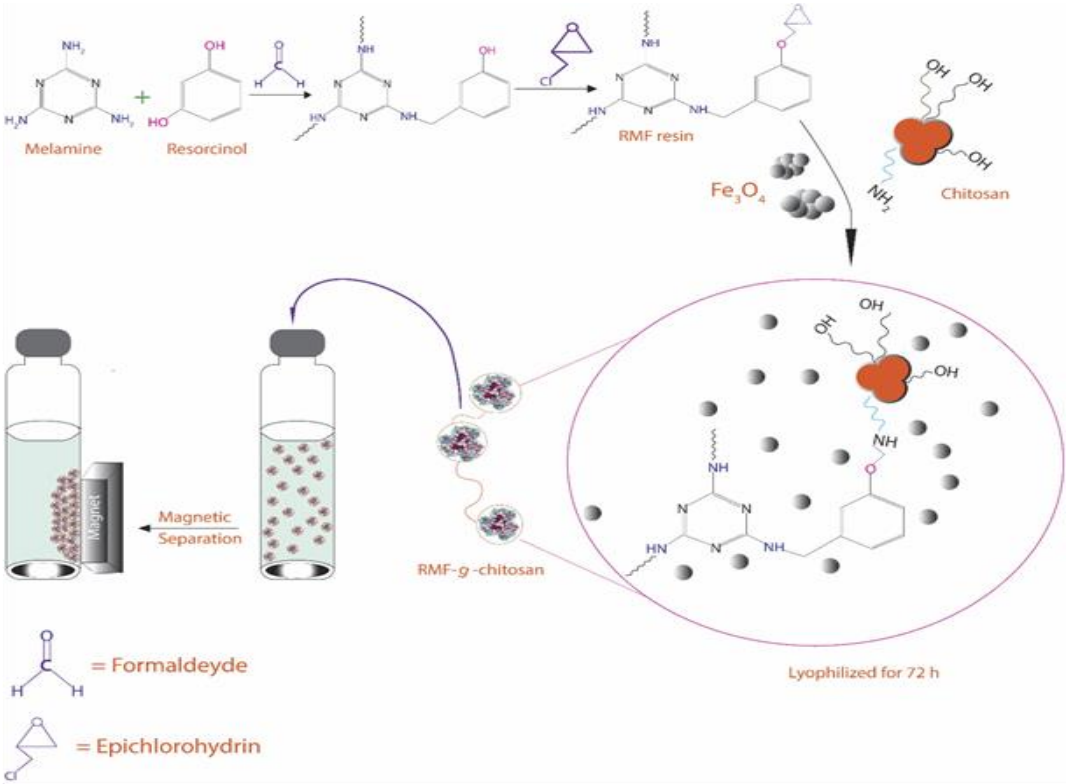

Scheme 4: Synthesis of magnetic resin grafted to chitosan porous bead (R-g-Ch)

3.2.4 Synthesis of magnetic mesoporous resin (m-RMF)

The magnetic mesoporous resin was synthesized in two steps according to the procedure depicted in scheme 5 below. To prepare the mesoporous RMF resin in the first step, Formaldehyde (8 ml), distilled water (42 ml) and ethanol (10 ml) were mixed in a 100 ml two-necked flask and heated to 85°C under stirring. Once the temperature attained 85^{o}C, melamine (4 g), resorcinol (4 g) and 2 g of nano-silica (used as a templating agent) were added to the above mixture before adjusting the pH to between 7- 8 using a 0.1M sodium carbonate solution. The mixture was then stirred at a constant temperature of 85^{o}C for 4 hours to ensure complete reaction. Thereafter, the pH of the mixture was decreased to the 3-4 range using concentrated HCl. The media

was then kept at 95 ^{o}C for 2 hours, with constant stirring. The solution was finally cooled to ambient temperature and precipitate obtained was rinsed using de-ionized water and dried in an oven at 60^{o}C.

In the next step, 4g of RMF mesoporous resin prepared above was added to a mixture of $(NH_4)Fe(SO_4)_2$.$6H_2O$ (1.5g), $FeCl_3$ (0.97g) in 300 ml of distilled water under nitrogen gas, and stirred at room temperature. The temperature of the mixture was gradually increased to 90^{o}C before adding 30 ml of NH_3.H2O (28% w/w) solution dropwise until the pH of 10-11 was reached. Following vigorous stirring for 1 hour, the mixture was cooled to ambient temperature; precipitate m-RMF obtained was rinsed and dried. Finally, in order to remove the silica particles from the resin to create a porous resin, 50 ml of sodium hydroxide solution (10% w/v) was added onto the magnetic RMF resin. The porous m-RMF resin obtained was rinsed with distilled water and dried at 80^{o}C.

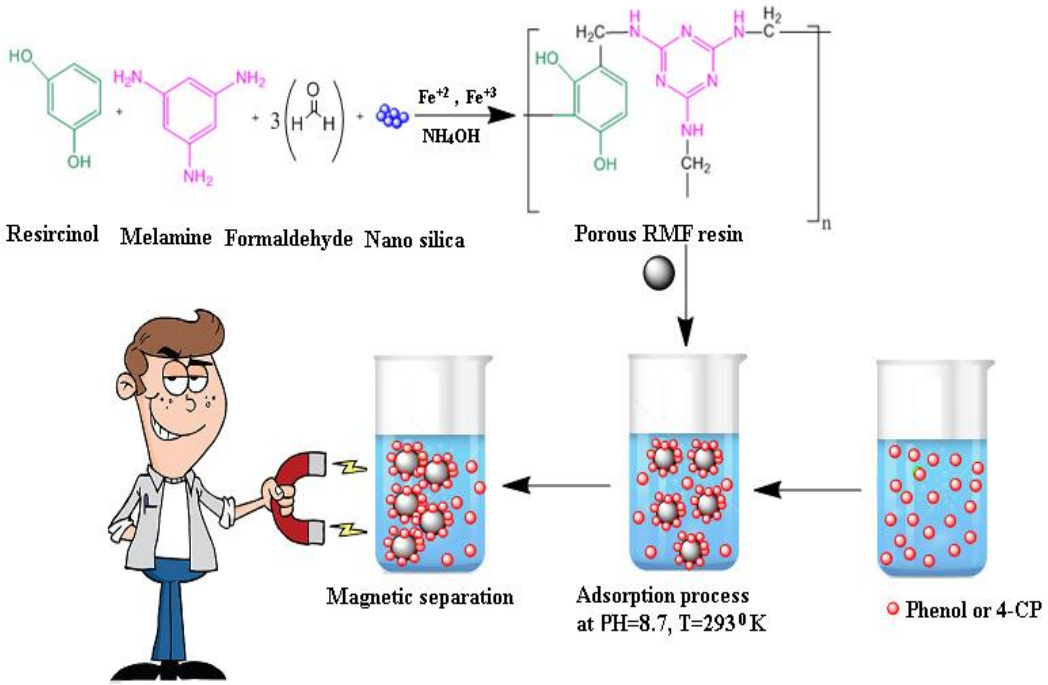

Scheme 5: Synthesis of m-RMF

3.3 Characterization and instruments

The presence of surface functional groups on the samples was investigated by Fourier Transform Infrared (FTIR) spectroscopy in the range of 400–4000 cm^{-1} using a spectrometer supplied by PerkinElmer (Waltham, MA, USA) at room temperature. The surface morphology of the sample was obtained using a scanning electron microscope JSM-6300 (JEOL, Japan). The pH point zero charge (pH_{pzc}) is an important surface property that characterized the pH at which the surface of an adsorbent exhibit net electrical neutrality. Herein, the pH_{pzc} of all samples was determined by the pH drift method [191-193]. Thermal degradation behavior of both samples was investigated using a thermal gravimetric analyzer (STA7300, HITACHI, Japan). A Perkin Elmer Spectrophotometer (LAMBDA 365) was used to determine the concentration of phenolic compounds while a Lyophiliser (MartinChrist alpha 1-2 LD plus, Germany) was used to produce porous magnetic resin chitosan beads. X-ray diffraction analysis of Fe_3O_4 nanoparticles (a), RMF (b) and m-RMF(c) was obtained by the powder method on a Rigaku Dmax2200PC diffractometer (Rigaku Corporation, Tokyo, Japan) equipment using Cu Kα-radiation. The diffraction pattern in the range of $5^\circ \leq 2\theta \leq 90^\circ$ was measured with a scan speed of 2° min^{-1}. The phases in the samples were compared with the standard JCPDS-ICDD files [207]. The specific surface area, volume and pore size analysis were carried out by Brunauer-Emmett-Teller (BET) methods. To investigate magnetic properties, a vibrating sample magnetometer (VSM, 7400, Lakeshore, USA) was applied at 25 ^oC. The magnetic behavior of m-RMF at room temperature before and after adsorption experiments were recorded using a VSM with an applied magnetic field of -10,000 to 10,000 Oe.

3.4 Adsorption equilibrium experiments

Batch experiments were carried out to study the effect of various parameters (dosage, pH, initial concentration, temperature, and time) on the adsorption equilibrium experiment of both adsorbents for the removal of phenol and 4-CP. Stock and working solutions of Phenol and 4-CP aqueous solutions were prepared by using deionized water.

3.4.1 Batch adsorption studies of R-g-Ch

The batch experiments were performed to investigate the adsorption behavior of R-g-Ch. An aqueous stock solution of the adsorbates was prepared by mixing an appropriate amount of 4–CP (molecular weight, Mw = 128.6) and phenol (Mw = 94.1) with deionized water. pH of the solution was adjusted using required volumes of 0.1 N NaOH and/or 0.1 M HCl before adding the adsorbent. In brief, 0.3 g of R-g-Ch was added to 100 ml volumetric flasks containing 25 ml of phenolic compounds (phenol or 4–CP solution) at constant temperature and pH. The suspension was shaken on a thermostat shaker at 100 rpm to attain equilibrium. Periodically, the R-g-Ch was separated from the reaction flask by an external magnet and the supernatant concentration was determined by a UV–vis spectrophotometer at the calibrated maximum wavelength of 244 and 280 nm for phenol and 4–CP, respectively. Series of experiments were performed to investigate the effects of initial pollutant concentration (10–200 mg/L), R-gCh dosage (0.1–0.6 g), solution pH (2−12) and temperature (25 – 45 °C). Adsorption isotherm and kinetic studies were conducted by varying the initial adsorbate concentrations and reaction time at the optimal pH and R-g-Ch dosage respectively.

All measurements were repeated at least 3 times and average results reported with the relative standard deviation of 3%. The equilibrium adsorption capacity of R-g-Ch was calculated using equation (1):

$$q_e = \frac{(C_0 - C_e)}{m} V \quad (1)$$

Where q_e is the equilibrium amount of adsorbate (mg/g) adsorbed; C_o is the initial concentration in mg/L, C_e (mg/L) is the equilibrium concentration of adsorbate, V is the volume of the aqueous solution (L) and m is the mass (g) of adsorbent beads used in the experiment.

The amount of phenol and 4-CP uptake by the magnetic porous bead in each flask at pre-determined time intervals was calculated using the following relationship equation (2):

$$q_t = \frac{C_o - C_t}{m} V \quad (2)$$

Where q_t is the adsorption amount in mg/g at contact time (*t*), C_o is the initial concentration of adsorbate and C_t is its concentration at any time *t*; V (L) is the volume of solution and m is the amount of dry adsorbent.

3.4.2 Batch adsorption studies of mesoporous RMF

Similar batch adsorption experiments to R-g-Ch were also conducted to examine the adsorption behavior of the adsorbates on m-RMF. Briefly, 0.1 g of m-RMF was added to 50 mL volumetric flasks containing 25 mL of the phenolic compounds (phenol or 4-CP solution). Series of experiments were performed where the initial adsorbate concentration was constant (10 mmol/l) at varying pH values (2-10) to determine the optimum pH for phenol removal. The adsorption experiments were carried out at room temperature (25^{o}C) under continuous stirring at 100 rpm unless otherwise stated.

Periodically, the m-RMF was separated from the reaction flask by an external magnet and the supernatant concentration was determined by a UV-vis spectrophotometer (PerkinElmer, USA) at the calibrated maximum wavelength of 244 and 280 nm for phenol and 4-CP, respectively. Adsorption isotherm and kinetic studies were conducted with initial adsorbate concentrations ranging from 1-10 mmol/l and varied reaction time (1 - 45 min) at the optimal pH, respectively. Each experiment was performed in triplicate and average results reported with the relative standard deviation of less than 3%. The equilibrium adsorption capacity of m-RMF was calculated using equation (1) above to determine the equilibrium amount of adsorbate (mmol/g) adsorbed per gram of the adsorbent.

3.4.3 Porosity of R-g-Ch

The porosity of R-g-Ch was determined by a gravimetric method using equation (3). In this method, ethanol was used as the displacing solvent since it penetrates into the pores of the beads without inducing swelling or shrinking of the matrix. The dry beads were initially weighed and then immersed into a certain volume of ethanol (V_1) in order to have the pores filled for 10 minutes. Therefore, there is a new volume (V_2) which contains the volume of ethanol and ethanol-impregnated into the porous beads. The beads were then removed from the liquid and the liquid on the surface was removed by employing filter paper. The volume of residual ethanol after the removal of the beads was denoted as V_3. The porosity of the beads was calculated as the total volume of the polymer beads, and the volume of ethanol within the porous beads.

$$\text{porosity} = \frac{V_1 - V_3}{V_2 - V_3} \times 100 \qquad (3)$$

The experiments were carried out 5 times and the average porosity value was found to be ~ 62%.

3.5 Adsorption Isotherm

Adsorption isotherm studies was undertaken to find the equilibrium relationship between the amount of a substance adsorbed at constant temperature and its concentration. In this study, the Langmuir and Freundlich isotherm models were applied to understand the experimental sorption behavior of both adsorbents [190].

The Langmuir model assumes that a monolayer surface adsorption on the adsorbent is favorable while the Freundlich model proposes the contribution of heterogeneous energy distribution during multilayer surface adsorption. In this current investigation, linearized forms of the Langmuir and Freundlich isotherm models (equations 4 and 6) were applied to better understand the equilibrium data of the adsorption of the phenolic compounds by both the mesoporous magnetic resin m-RMF and the R-g-Ch beads.

$$\frac{C_e}{q_e} = \frac{C_e}{q_m} + \frac{1}{K_L \cdot q_m} \qquad (4)$$

Where q_e (mg/g) is the adsorption capacity on adsorbent at equilibrium, C_e (mg/L) is the equilibrium concentration of the adsorbate in solution, q_m is the maximum adsorption capacity in mg/g and K_L is the Langmuir constant or rate of adsorption (L/mg). q_m and K_L can be calculated from the slope and intercepts of the straight line graph obtained when C_e/q_e was plotted against C_e. The Langmuir parameters and the correlation coefficient (R^2) were calculated and are listed in Table 1. The dimensionless factor (R_L) in Langmuir isotherm which indicates the nature of the adsorption process can be calculated using equation 5.

$$R_L = \frac{1}{1 + K_L C_0} \qquad (5)$$

Where C_o (mg/g) is the initial concentration of phenolic compound and K_L (L/mg) is the Langmuir constant. The R_L value indicates that adsorption tend to be favorable ($0 < R_L < 1$), unfavorable ($R_L > 1$), linear ($R_L = 1$) and irreversible ($R_L = 0$). The R_L values obtained in our study is also listed in Table 1 and shows that the adsorption behaviors of both adsorbents were favorable for the phenolic compound ($0 < R_L < 1$).

The linear form of the Freundlich equation is shown in equation 6 below [192, 196]:

$$\ln q_e = \ln K_f + \frac{1}{n}\ln C_e \quad (6)$$

Where, K_F (mg/g) (L/mg) and 1/n are Freundlich constants that represent the adsorption capacity and adsorption intensity of the adsorbent. The values of K_F and 1/n can also be determined from the intercept and slope of the linear plot of *In* q_e versus *In* C_e. The value of 1/n predicts if the adsorption is favorable when $0 < 1/n < 1$, not favorable when $1/n > 1$ and irreversible if $1/n = 0$.

3.6 Kinetic study

To further explain the adsorption behavior of the phenol and 4–CP on both adsorbents, the experimental data were fitted to the intra-particle diffusion, pseudo-first order, pseudo-second-order kinetic models and are presented in Table 1. The correlation coefficient (R^2), average relative error (ARE) and the calculated adsorption capacity of the adsorbate ($q_{e,\ cal}$) were used to determine the applicability of the adsorption kinetics model. The linearized-integrated form of pseudo-first, pseudo-second order, and intra-particle diffusion equations are given in equations 7- 9 respectively [192]:

$$\text{In}\ (q_e - q_t) = \text{In}\ q_e - K_1 t \quad (7)$$

$$\frac{t}{q_t} = \frac{1}{K_2 q_e^2} + \frac{t}{q_e} \quad (8)$$

$$q_t = K_{id} t^{0.5} + C \quad (9)$$

Here, the q_t and q_e (mg/g) are the amounts of adsorbate adsorbed by the adsorbents at any time *t* and equilibrium time (min) respectively. The k_1, k_2, and k_{id} represent the kinetic rate constants for each model accordingly.

3.7 Thermodynamics of the adsorption

The thermodynamic study was performed to determine the feasibility and nature of the adsorption process. Equation 10 was employed to calculate the different thermodynamic parameters (ΔH°, and ΔS°).

$$\ln K_d = \frac{\Delta S^o}{R} - \frac{\Delta H^o}{RT} \qquad (10)$$

Where, R is the gas constant (8.314 J/mol K), T is the absolute temperature in Kelvin and K_d is the equilibrium constant that was obtained from the Langmuir equation. The values of ΔH° and ΔS° were obtained by plotting a graph of ln K_d vs 1/T. The Van't Hoff equation $\Delta G° = \Delta H° - T\Delta S°$ was employed to calculate the values of ΔG°. −ΔG° values indicate the adsorption process to be feasible and spontaneous in nature. +ΔS° values describes the randomness at the solid-solution interface during the adsorption process while −ΔH° value suggests an exothermic nature of adsorption [196].

Chapter 4

RESULTS AND DISCUSSION

4.1 Characterization of polymers

4.1.1 SEM analysis of m-RMF

The SEM image of the m-RMF surface morphology is presented in Figure 1. The investigation reveals a smooth surface and sphere-like morphology with plenty of pores distributed on the surface of the material. This confirms that we were able to achieve a mesoporous material which is the focus of the present study. Average size of m-RMF was determined to be 20nm.

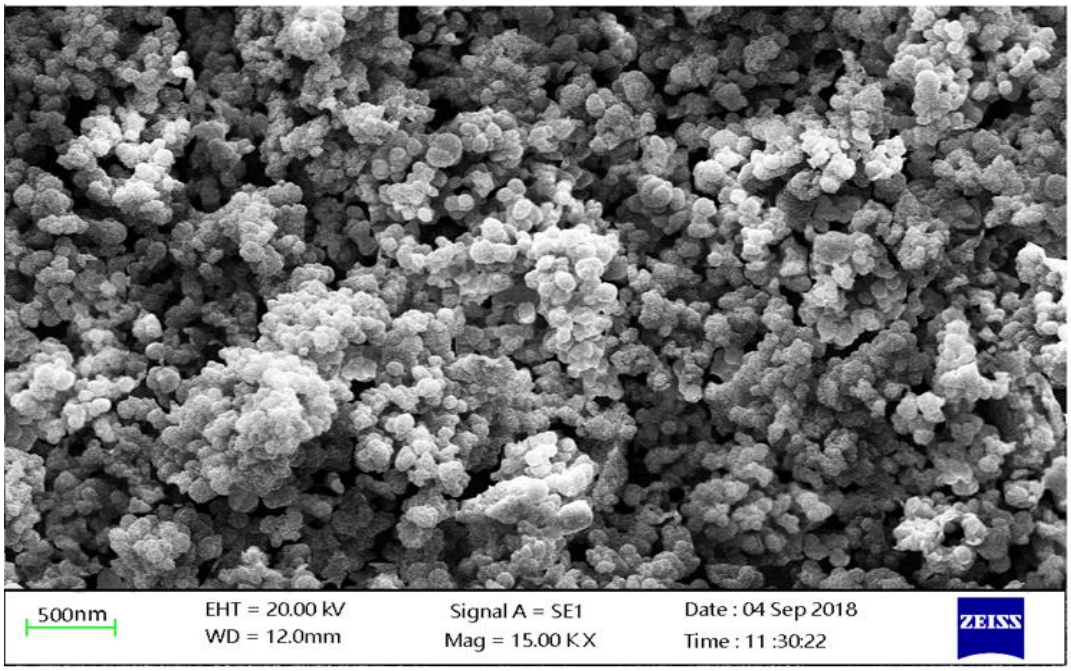

Figure 1: SEM image of m-RMF

4.1.2 SEM analysis of R-g-Ch

The morphology of the R-g-Ch was investigated by a Scanning Electron Microscopy (SEM) using a JSM-6300 (JEOL) microscope (Figure2). It is noted that the light brown wet spherical shaped R-g-Ch beads turned into dark brown quasi-sphere after successive freeze-drying. This is probably due to the condensation reactions and partial oxidation of the magnetic moiety (Fe_3O_4) surface during the freeze-drying process. The dried R-g-Ch beads have an average diameter of ~2.9 mm and the outer surface morphology exhibited fiber-like interconnected porous network with varying meso and macropore sizes, which would facilitate diffusion of the selected adsorbates into the adsorptive sites.

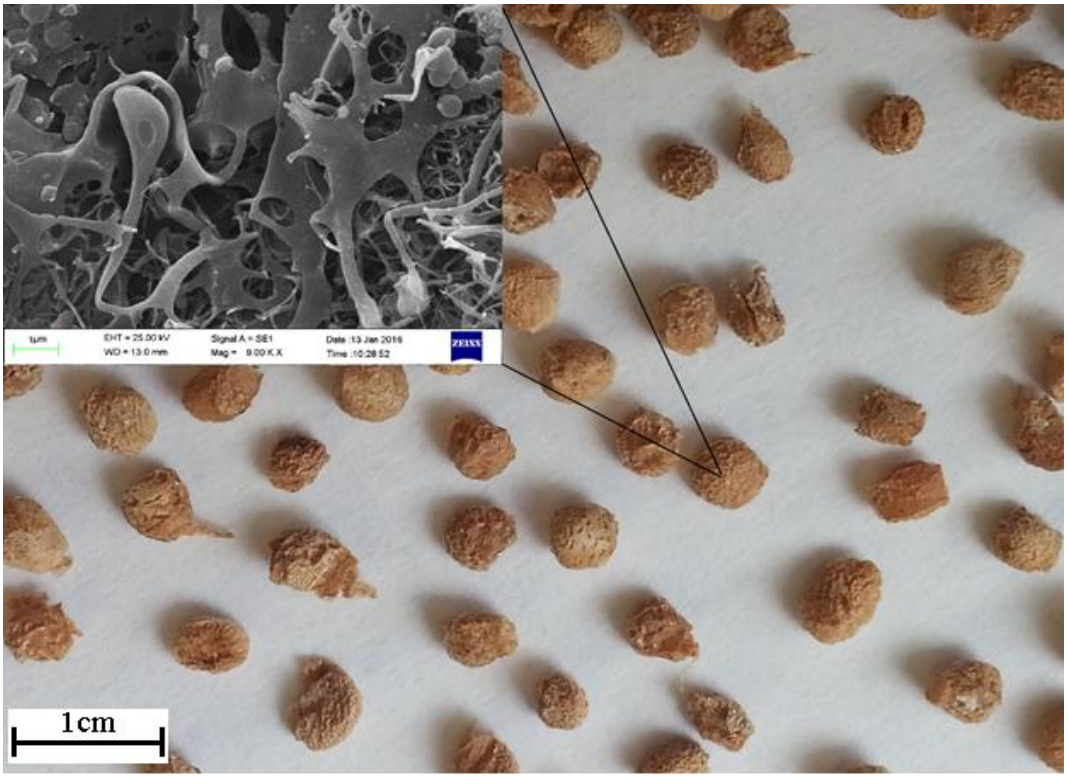

Figure 2: SEM image of magnetic resin grafted chitosan porous bead (R-g-Ch)

4.1.3 FTIR analysis m-RMF

Fig.3 shows the FTIR spectra of the monomers (resorcinol and melamine) and magnetic resin (m-RMF) synthesized. The broad peaks around 3600-3450 cm^{-1} in all the samples are attributed to the strong –OH bonding which overlaps the weaker –NH or $–NH_2$ stretching vibrations (3400-3280 cm^{-1}) [196]. The peaks at 2970-2950 cm^{-1} are assigned to the asymmetric stretch vibrations of C-H in CH_3 groups. Peaks corresponding to typical –C=C– were observed at 1600 cm^{-1} [198]. Specifically, the weak N-H amines can be seen for the melamine spectra at 3493 cm^{-1} [188]. The C=N stretch vibrations show low band for melamine compound at 1618 cm^{-1}, while two sharp absorption peaks noticed at 1558 and 1230 cm^{-1} is attributed to the aromatic C−N stretching in the triazine unit and the triazine aromatic ring bending was observed at 810 cm^{-1} [199].

The m−RMF spectrum shows similar peaks in the fingerprint region as those of resorcinol and melamine, however, a new medium band at 534 cm^{-1} is observed which is indicative of Fe−O due to the introduction of Fe_3O_4 (magnetite) [189].

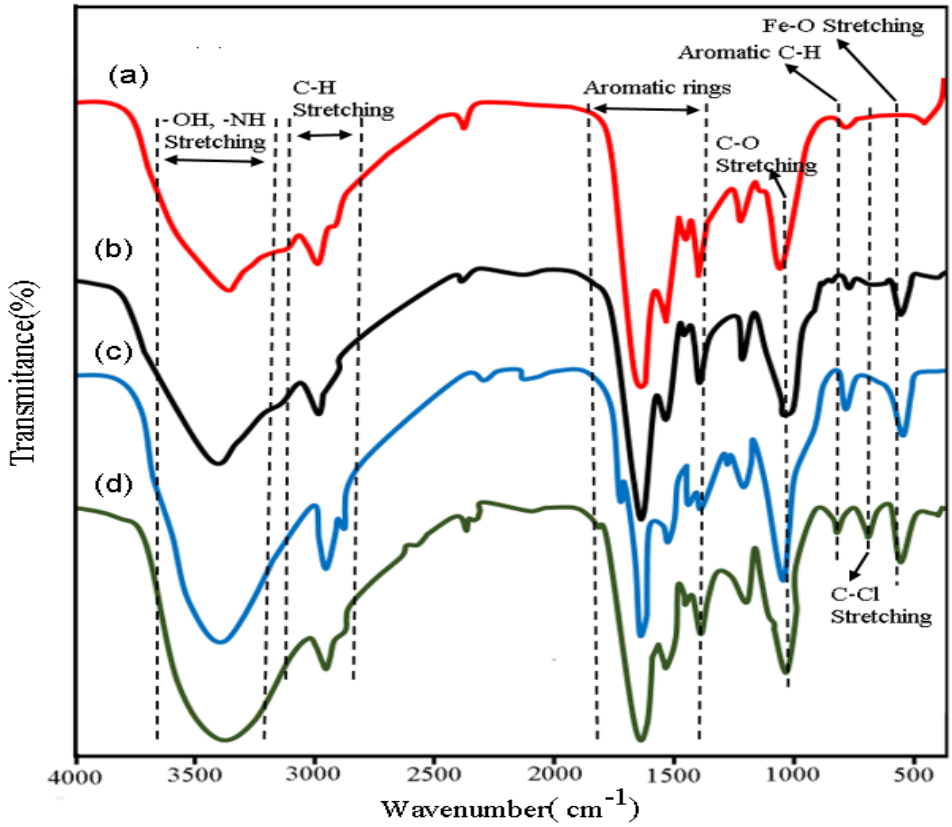

Figure 3: FTIR spectra of resorcinol, melamine and m-RMF

4.1.4 FTIR analysis R-g-Ch

Figure 4 on the other hand shows the FTIR spectrum of the R-g-Ch, resorcinol, melamine, and RMF. All the spectra possess strong and broad bands in the 3700-3100 cm^{-1} region, which is assigned to –OH bond stretching. The band overlapped the weaker –NH or $–NH_2$ stretching vibrations (3400-3280 cm^{-1}). The slight peaks at 2968-2940 cm^{-1} are assigned to the stretch asymmetric vibration of C-H in CH_3 groups [200]. The peaks corresponding to typical C-C and C-N were observed at 1600-1620 cm^{-1} in the resorcinol and melamine spectra.

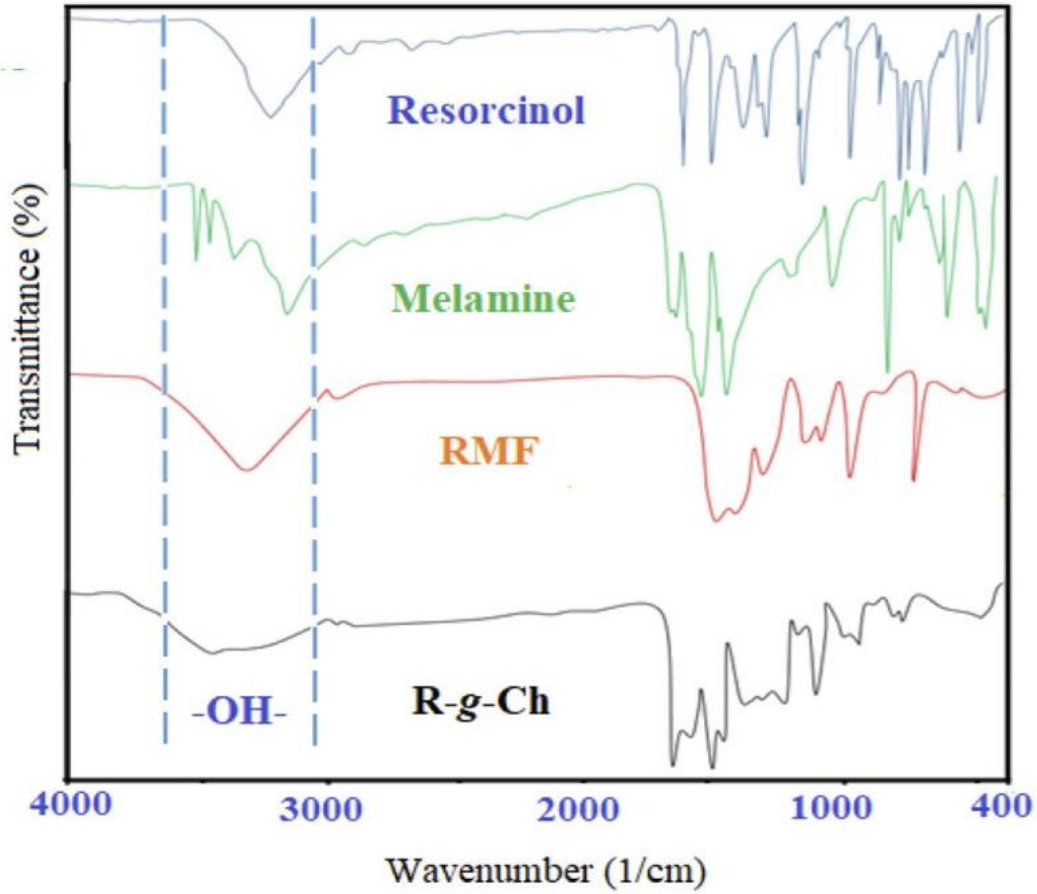

Figure4: FTIR spectra of Resorcinol, Melamine, RMF, EPC-RMF, R-g-Ch

4.1.5 TGA/DTA analysis m-RMF

The TG and DTG curves of m-RMF are shown in Figure 5. The continuous and dashed lines represent the TG and DTG curves respectively. TG diagram of m-RMF shows a slight weight loss (2.3%) below 24^{o}C. This may be due to the water molecules that vaporized from the absorbent surface. Further weight loss between 365 and 800^{o}C is probably attributed to the decomposition of melamine moieties. The DTG curve shows a strong exothermic peak at 410^{o}C due to decomposition of resin structure.

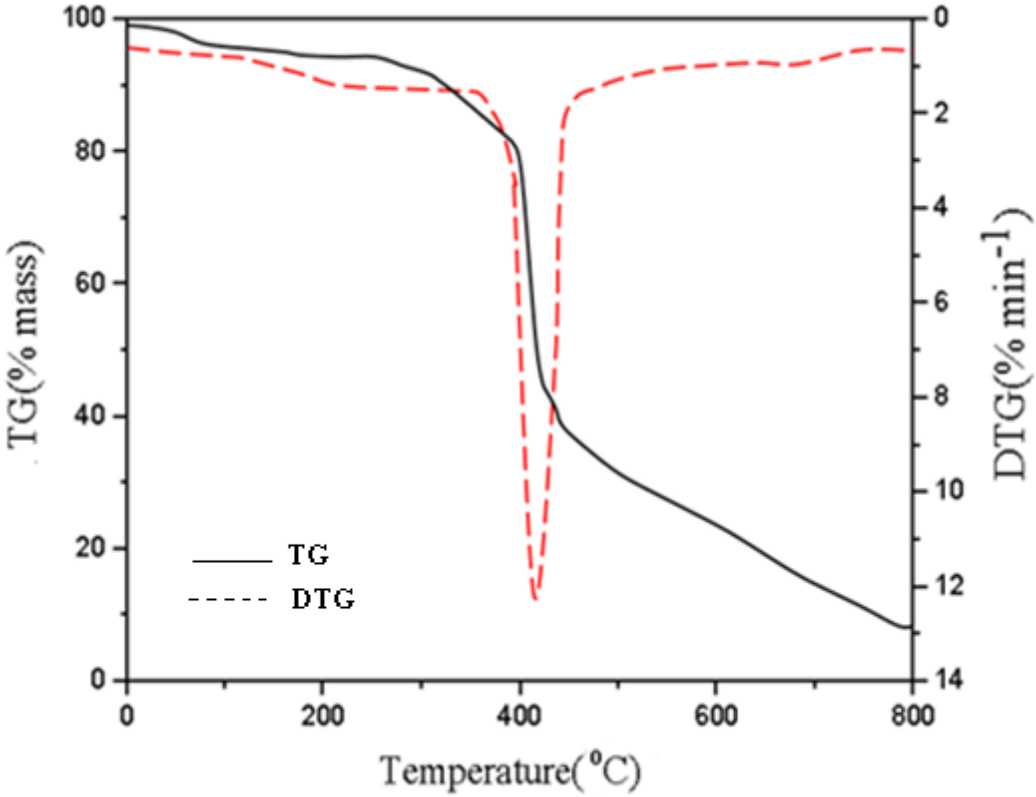

Figure 5: TG and DTG of m-RMF

4.1.6 TGA/DTA analysis R-g-Ch

Figure 6. Shows the TG and DTG thermograms of the R-g-Ch beads. The continuous and dashed lines represent the TG and DTG curves respectively. The TG curve exhibited four distinct weight loss stages in the region of 75-750°C. At the first stage, a slight curvature was observed which indicated a 5.7% loss of weight and mainly attributed to the vaporization of absorption water molecules present (75-130°C). A 50.4% weight loss in the second stage is attributed to the decomposition of chitosan and notably shown in the flexion in DTG curve (Tpeak = 327°C). The degradation of the RMF resin occurred at the 3rd stage within the range of 315-560°C [200]. 8.4% weight loss in the last stage (560-665°C) is related to the cleavage and composition of melamine [203].

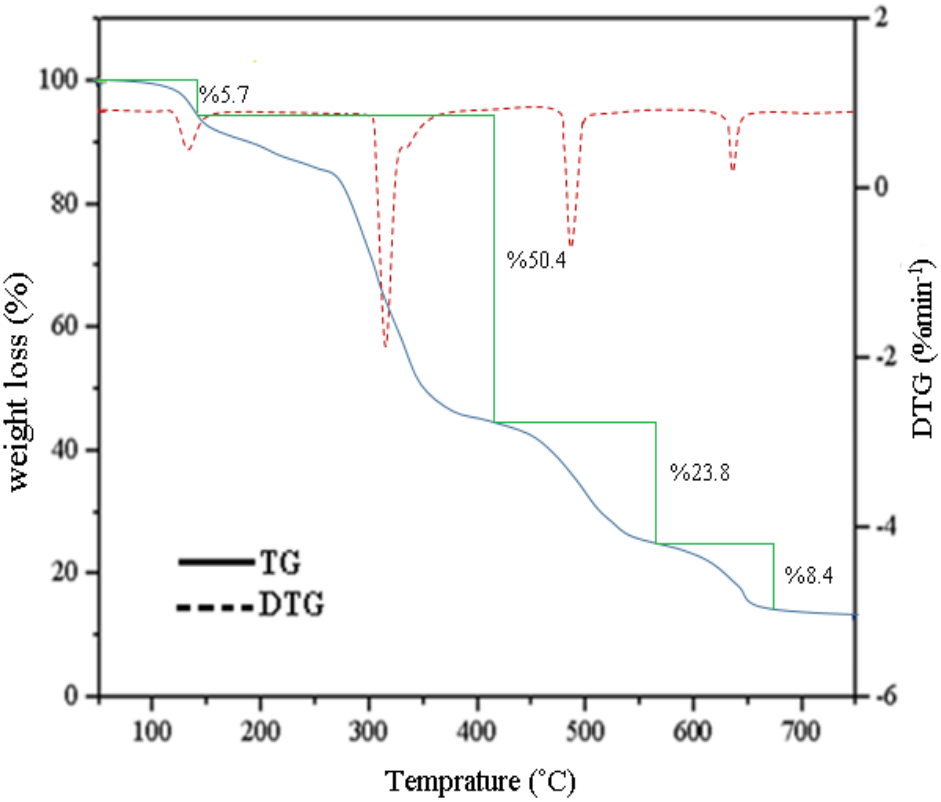

Figure 6: TG and DTG curves of R-g-Ch

4.1.7 Structural property of m-RMF

Figure 7 shows the N_2 adsorption-desorption isotherms for m-RMF. As clearly seen, m-RMF exhibited reversible type IV isotherm with H_3 hysteresis and large N_2 uptake at p/po ≥ 0.70, which is typical of porous materials [204]. At maximum relative pressure, there is a hysteresis loop which has the mesopores size (2-50 nm) according to the IUPAC pores classification. As indicated in the inset in Fig. 7, m-RMF exhibits a wide pore size dispensation in the limit area of 5-10 nm (mesopores) [205], suggesting that the m-RMF internal mass transfer resistance for phenol and 4-CP is negligible [198, 206].

It is observed that the N_2 quantities adsorbed by m-RMF at p/po ≥ 0.85were higher, hence, suggesting a high specific surface area and uniform dispensation of mesopores

on the surface of the m-RMF [202]. According to the BET analysis, the m-RMF possesses a specific surface area and the pore size was preconceived using the BrunauerEmmett-Teller (BET) and Barrett-Joyner-Halenda (BJH) methods[201, 202], respectively. The adsorption indicates that the Brunauer-Emmett-Teller (BET) surface area, the pore volume, and the average pore diameter were 520 m^2/g, 0.45 cm^3/g and 3.5 nm respectively.

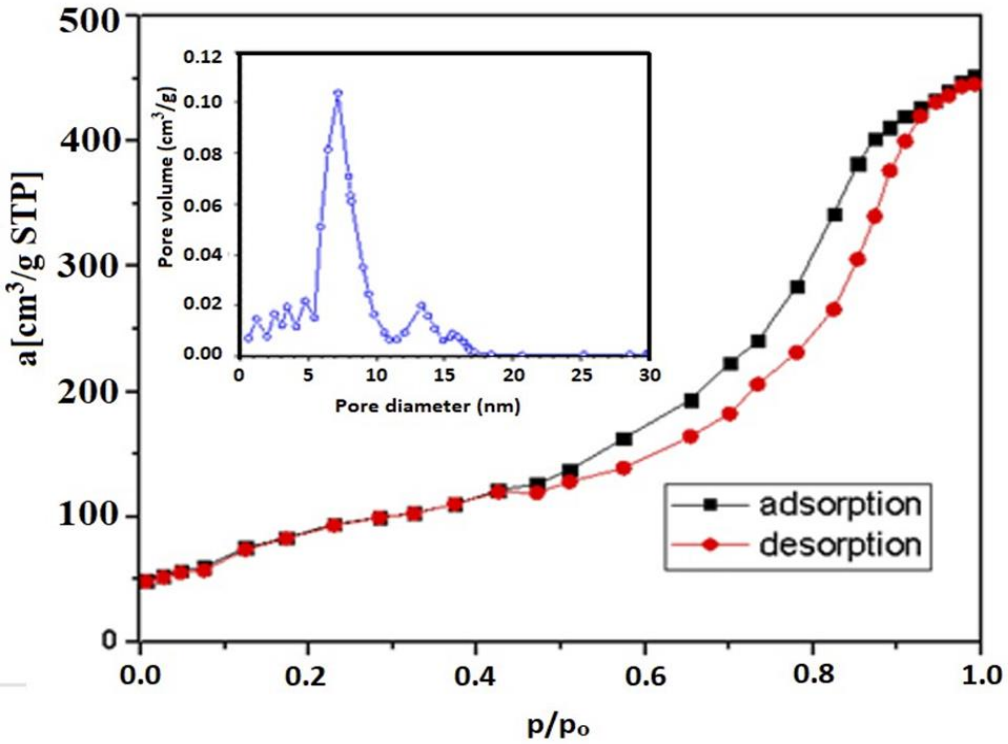

Figure 7: N_2 adsorption and desorption of m-RMF

4.1.8 VSM pattern nanoparticles of m-RMF

The magnetic behavior of m-RMF at room temperature before and after adsorption experiments were recorded using a VSM with an applied magnetic field of -10,000 to 10,000 Oe at Figure 8. The values of the saturation magnetization (Ms) of m-RMF before adsorption are 30.2 emu/g, 9.9 emu/g and 86.4 Oe, respectively. After adsorption of phenol, the corresponding magnetic parameters were slightly decreased.

The 26.4 emu/g, 9.2 emu/g and 79.6 Oe were obtained for Ms, Mr and Hc after adsorption of phenol by m-RMF and similar results were obtained after 4-CP adsorption. Hence, results herein indicated that the magnetic moiety (Fe_3O_4) in the m-RMF does not only confer magnetic properties on the RMF but also participated in the adsorption of the adsorbates. A similar trend has been observed in our earlier reports [205, 193].

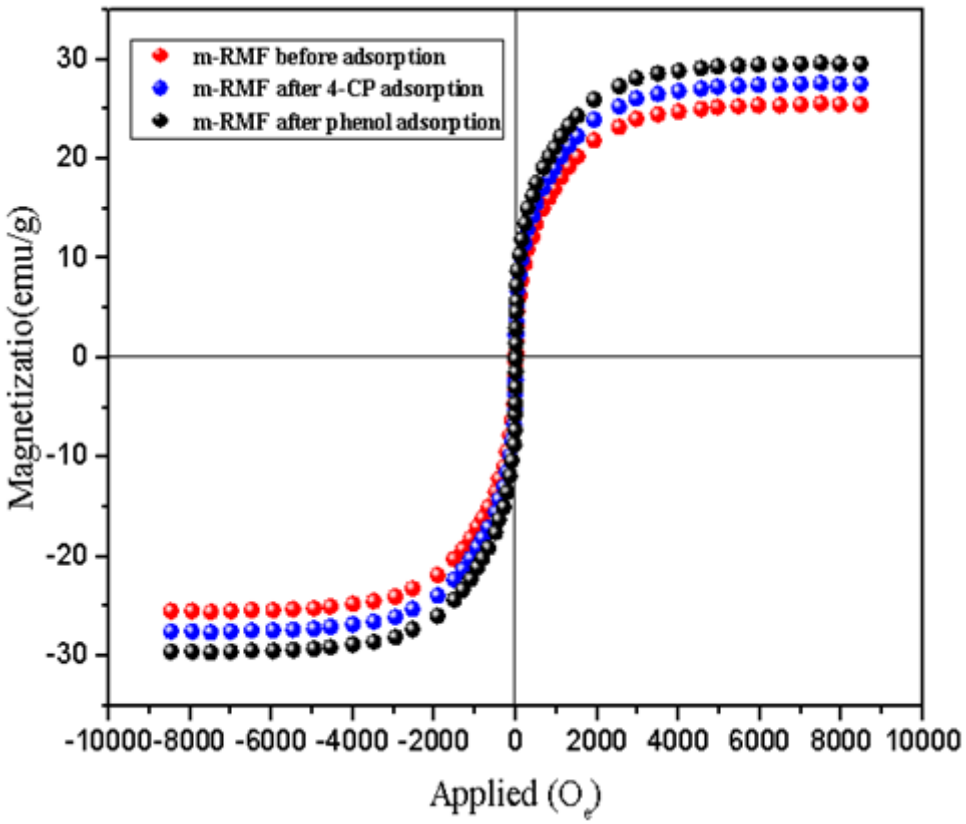

Figure 8: Vibrating samples magnetometer (VSM) curves of Fe_3O_4, m-RMF at room temperature.

4.1.9 XRD characterization of m-RMF

The XRD diffraction was applied to detect the compound present in the resin. As shown in Figure 9., The XRD pattern of Fe_3O_4 and m-RMF nanoparticles show six characteristic peaks for Fe_3O_4 (2θ=30.2°, 35.6°, 43.3°, 53.5°, 57.2°, and 62.8°), and the peak positions could be indexed to (220), (311), (400), (422), (511) and (440),

respectively. Both peak position and the relative peak intensity suggest that the crystalline structure of the magnetite was essentially maintained. The diffraction peak with 2θ=22° could result from the amorphous m-RMF.

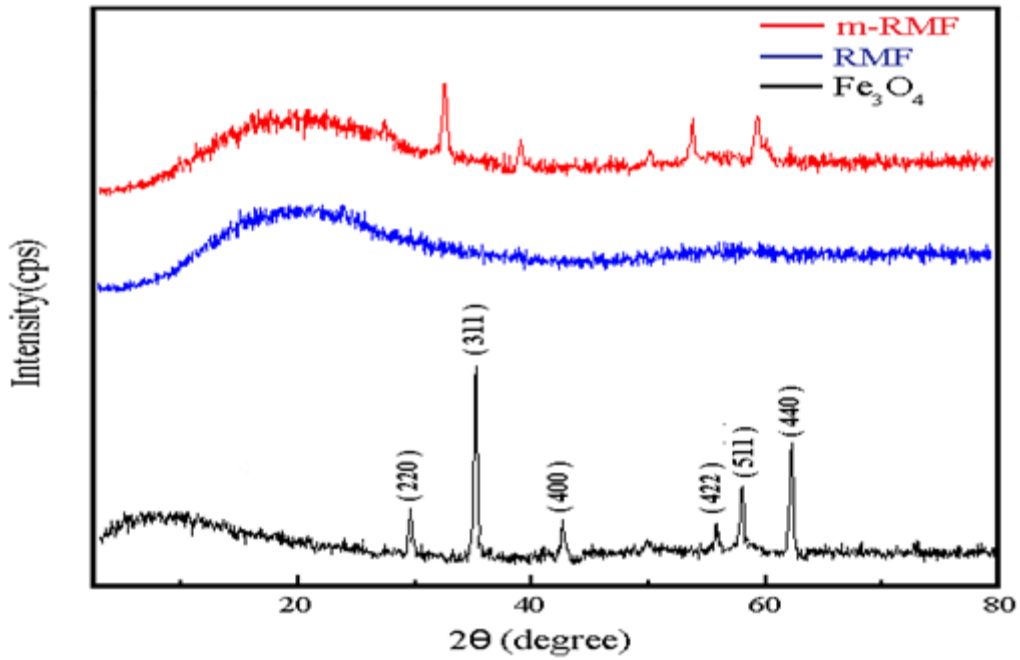

Figure 9: XRD pattern of magnetic Fe3O4 nanoparticle, RMF and m-RMF

4.2 Adsorption study

4.2.1 Effect of contact time of m-RMF

To understand the effect of time as a key factor in the adsorption process, the experiments were carried at different time intervals while evaluating the adsorption capacity of m-RMF. The results obtained are presented in Figure 10. It could be seen clearly from the figure that there was two-stage kinetic behavior before the adsorbent could achieve equilibrium adsorption. At the first stage, a fast adsorption rate from 1 to 30min was observed and at the second stage i.e. from 30 to 40 minutes, the adsorption was slow and reached to equilibrium. The initial fast rate of adsorption could be due to the large number of active vacant sites available for adsorption at the

initial stage. However, for the second stage, the process was slower and reached equilibrium since the number of active site on the adsorbent surface decreases with passing time during adsorption. Also, the repulsive forces created between phenolic compounds adsorbed on the surface of m-RMF and that remaining in solution i.e. bulk phase might also slow down or reduce the adsorption efficiency. Hence, optimum time of 45 minutes is sufficient to attain sorption equilibrium for both phenolic compounds.

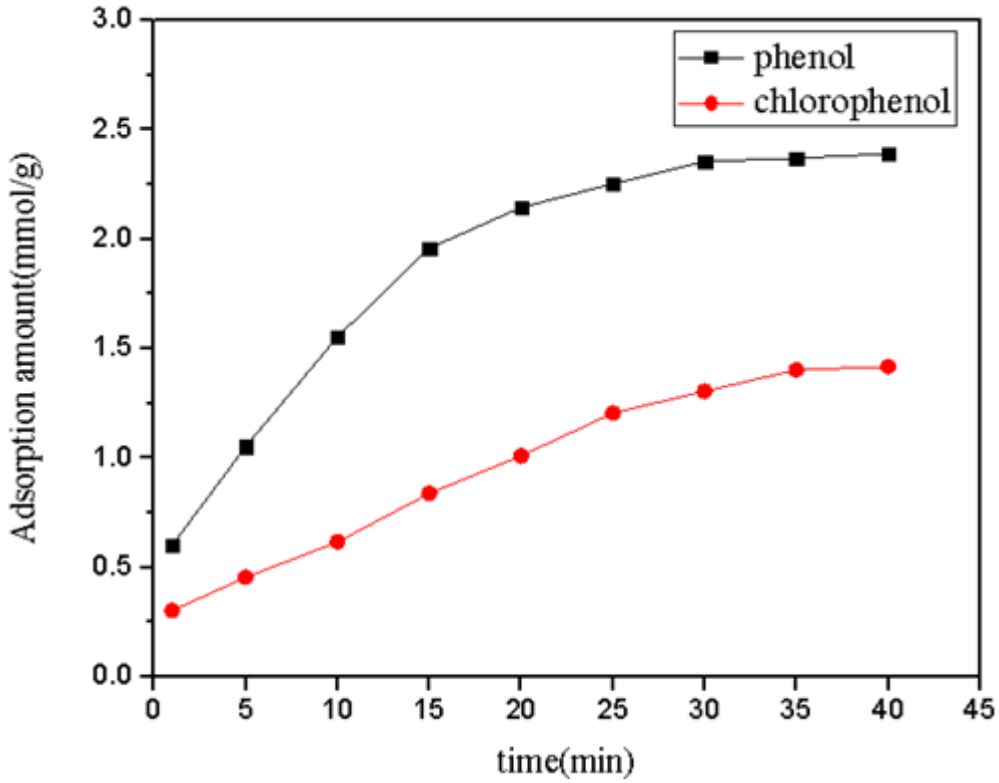

Figure 10: Effect of contact time on maximum capacity of phenolic compound by m-RMF

4.2.2 The effect of contact time of R-g-Ch

The contact time between adsorbent and adsorbate display a significant role on the adsorption process. The effect of contact time on the adsorption of phenol and 4-CP was studied under the optimized conditions. As shown in Figure 11, it can be seen that the rate of adsorption of phenol and 4-CP gradually increased with time until it reached

equilibrium adsorption. The equilibrium time was identical (700 min) for phenol and 4-chlorophenol.

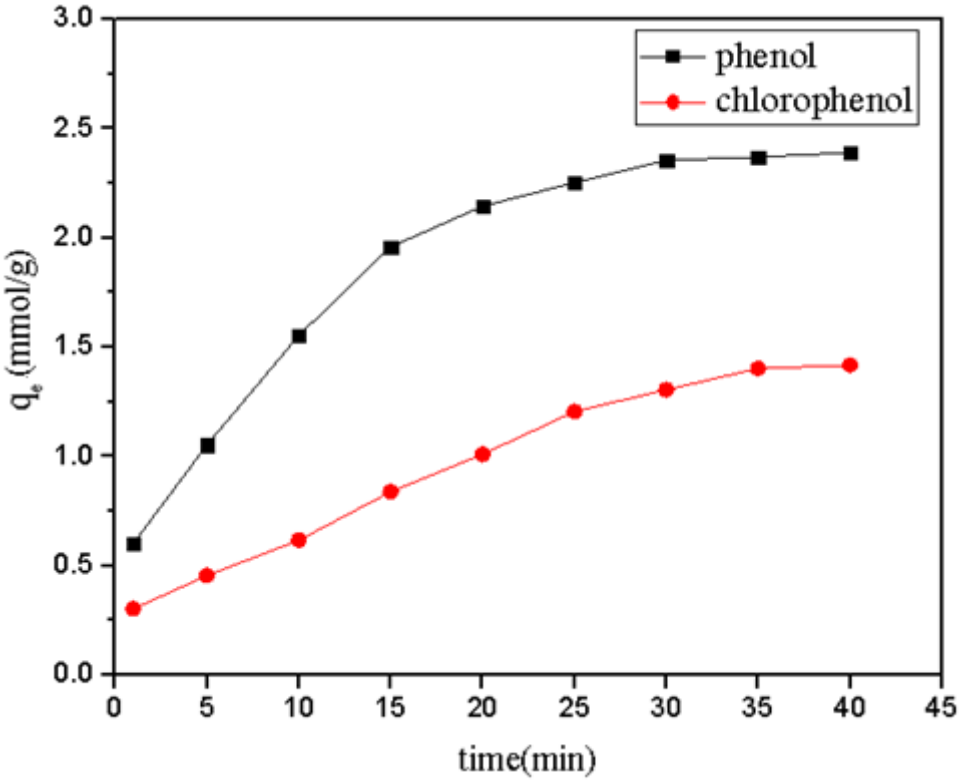

Figure 11: Effect of contact time on adsorption capacity of R-g-Ch

4.2.3 Effect of adsorbate dose of m-RMF

To investigate the effect of adsorbent dosage on the adsorption capacity of m-RMF, the dosage of m-RMF was varied (0.1-1g) and added to 25 ml of 10mmol/L phenolic compound at pH=8.7, 25^{o}C under constant shaking for 45min and represented in Figure12. The results revealed that an increase in the amount of the adsorbent decreased the adsorption capacity of both phenolic compounds on m-RMF. This is due to the concentration gradient or the split in flux between the solute concentration in the solution and that on the surface of the adsorbent. Thus, increasing the adsorbent dosage reduced the amount of phenols adsorbed per unit mass of adsorbent i.e. the active sites

present on the adsorbent surface was not fully utilized at higher dosage during the adsorption process. The optimum adsorbent dosage was found to be 0.1g.

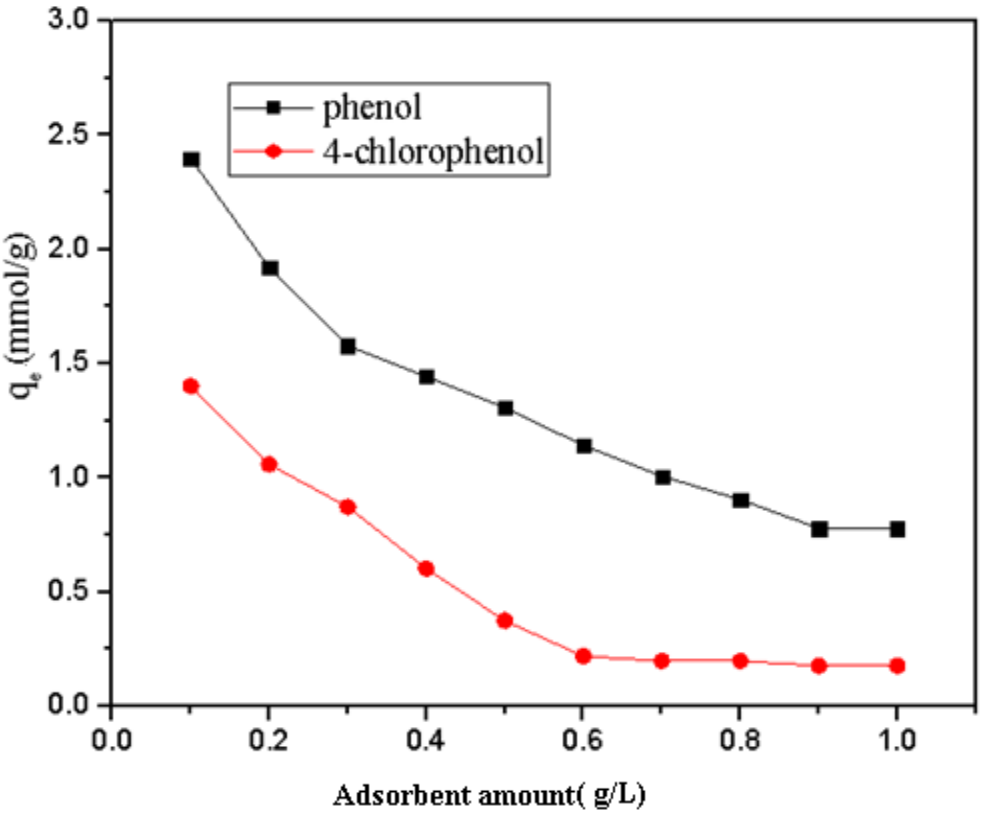

Figure 12: Effect of adsorbent dose on maximum capacity of phenolic compound by m-RMF

4.2.4 Effect of adsorbate dose of R-g-Ch

The adsorption behavior of phenol and 4-CP were investigated by varying the mass of R-g-Ch from 0.1- 0.6 g/L under optimum condition. The results were plotted and shown in Figure 13. As seen from the figure, adsorption of phenol and 4-CP increased with the increase in the dose of adsorbent. This might be attributed to the increase in available sorption surface and availability of more adsorption sites with increase in adsorbent dose. While adsorbent dose increased from 0.1 to 0.5 g/L, the adsorption capacity in turn increased steadily. However, there was no substantial increase in the

adsorption capacity as dosage was increased to 0.6 g/L hence subsequent experiments were conducted using 0.5 g of R-g-Ch beads.

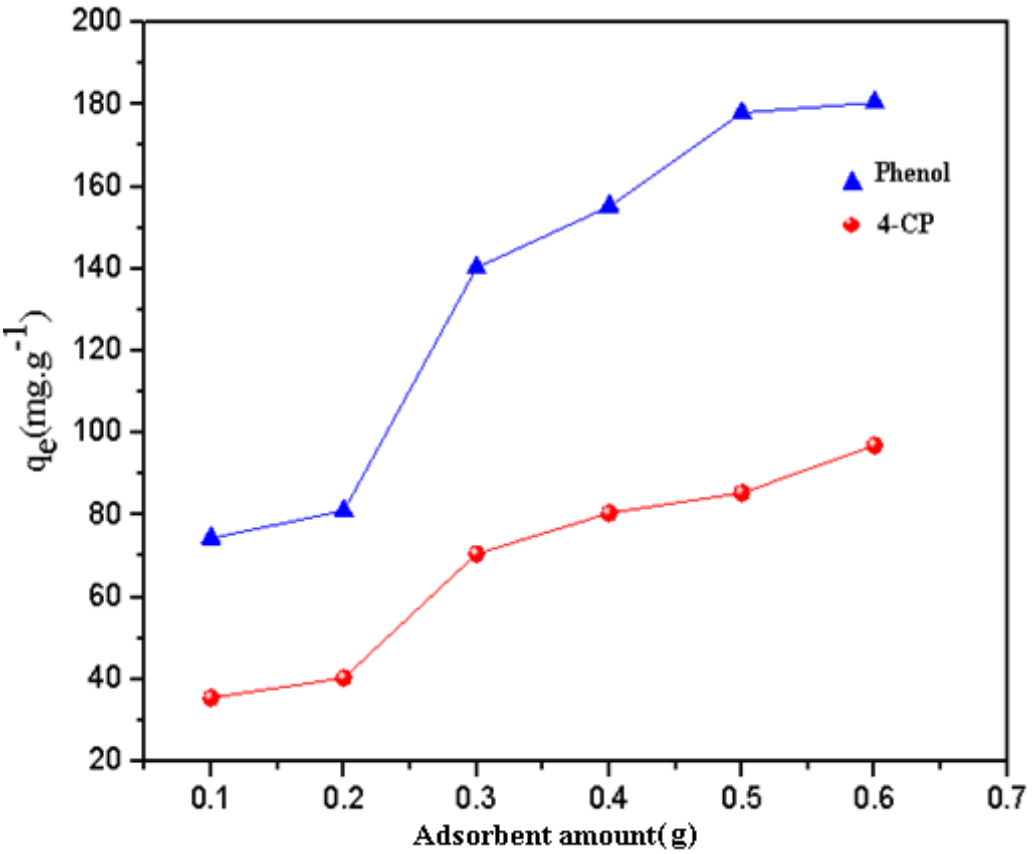

Figure 13: Effect of adsorbent amount on adsorption capacity of R-g-Ch

4.2.5 Effect of initial concentration of m-RMF

In order to consider the effect of initial concentration of phenol and 4-chlorophenol, 0.1 g of adsorbate was added to 25 ml of phenolic compound solution (1-10 mmol/L) in 50 ml volumetric flaks under stirring for 45 min, at 25^{o}C and optimum pH of 8.7. According to Figure 14, an increase in the initial concentration of both phenolic compounds led to a corresponding increase in the equilibrium adsorption amount for both phenols. This phenomenon is due to increase in the interaction and driving force between the adsorbate and active site of adsorbent. The optimum concentration of phenolic compound is found to be 10mmol/L.

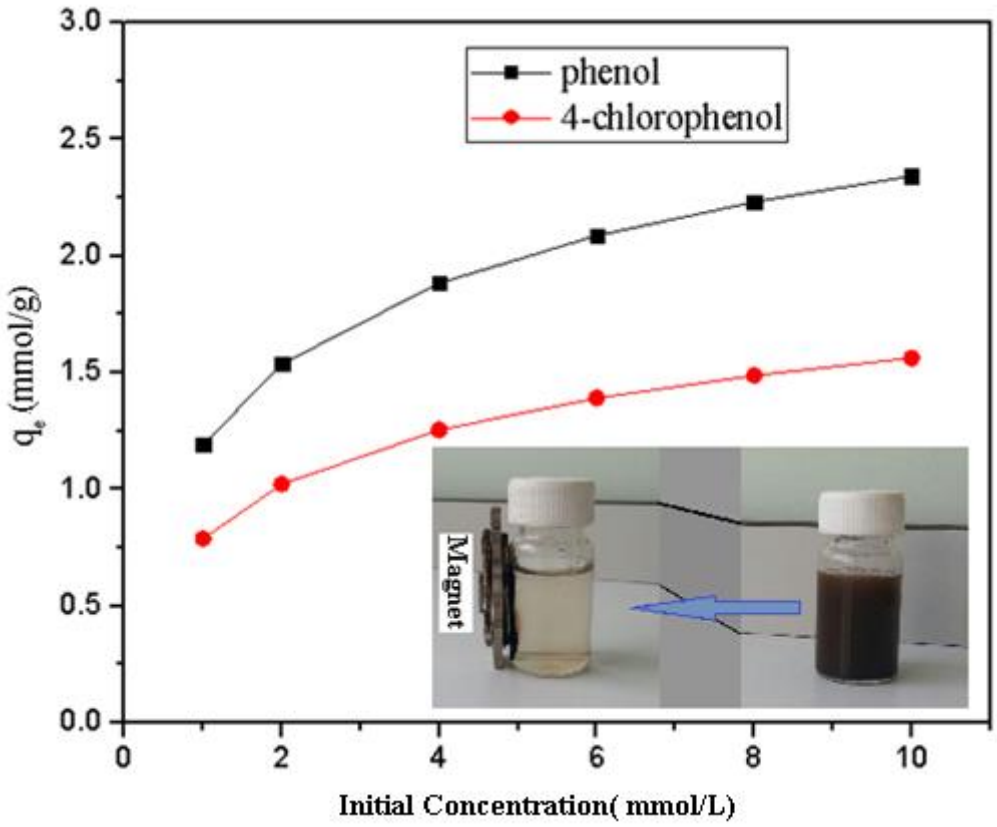

Figure 14: Effect of initial concentration on maximum capacity of phenolic compound by m-RMF

4.2.6 The effect of initial concentration of R-g-Ch

During the adsorption process, the effect of the initial concentration was investigated by varying the initial concentration of phenol and 4-CP from 10 to 200mg/l. Figure 15 shows that the adsorption capacity of the adsorbent increased with an increase in the initial phenol and 4-CP concentration. The adsorption capacity increased from 41.4 mg/g to 180.9 mg/g for phenol and from 12.06 to 95.5mg/g for 4-CP as initial concentration of both adsorbates increased from 10 to 200mg/l. This may be due to an increase in mass gradient between the solution and adsorbent, which acts as a driving force to overcome various mass transfer resistances of adsorbate molecules from bulk solution to the particle surface [208].

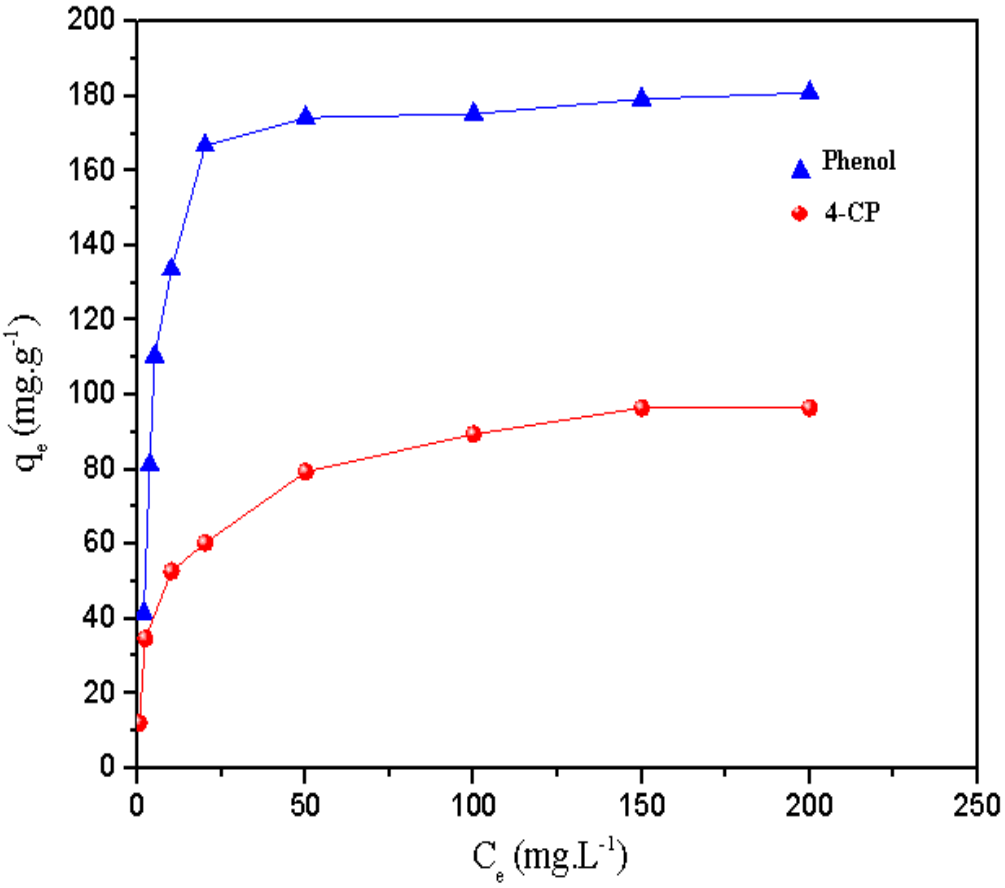

Figure 15: Effect of initial concentration on adsorption capacity of R-g-Ch.

4.2.7 The pH of Zero Point Charge of m-RMF

The pH point zero charge (pH_{zpc}) is an important surface property of a material that characterizes the pH at which the surface of an adsorbent exhibit net electrical neutrality. Here, the pH_{zpc} of m-RMF was determined by the pH drift method [193]. Briefly, a known amount of m-RMF was mixed in different pH (2-10) solutions and stirred for 24 h. Then, the final pH of the mixture was determined and plotted against the initial pH. The pH_{zpc} of the sample was taken as the point on the graph where $pH_{initial} = pH_{final}$. As seen in Figure 16, pH_{zpc} of m-RMF was found to be 7.8.

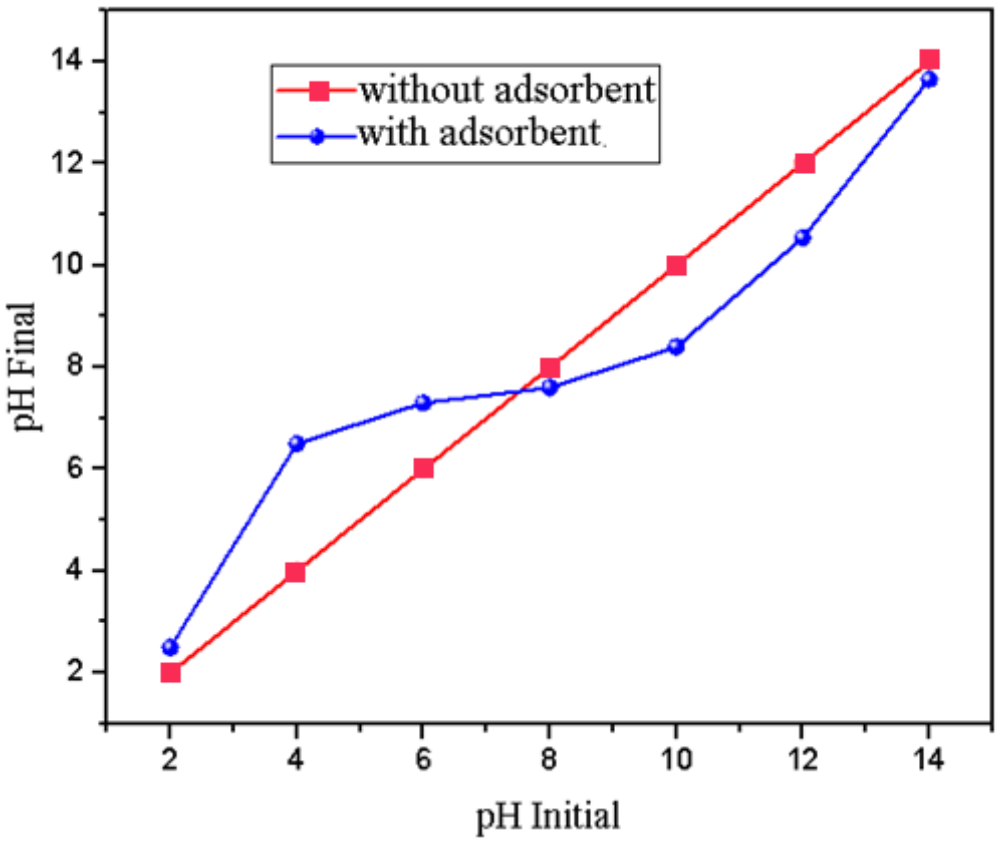

Figure 16: The Change of pH_{final} via pH_{initia}l for m-RMF (m = 0.1 g, V = 25 mL, and electrolyte concentration = 10 mmol/L)

4.2.8 Effect of solution pH of m-RMF

The removal capacity of m-RMF towards phenol and 4-CP with respect to changes in solution pH (1-11) is shown in Figure 17. The initial dose of m-RMF and initial concentration of the adsorbates at all pH values were 0.1 g and 10 mmol/L, respectively. Obviously, the adsorption process was pH-dependent and high removal capacity occurred at the alkaline condition. A similar trend has been reported in earlier researches.

In the pH range of 1- 9, the removal capacity of phenol and 4-CP increased steadily while a further increase in solution pH led to a decrease in the removal capacity of the adsorbent. Herein, it is concluded that the higher adsorption performance in alkaline

condition when compared to acidic condition is possibly related to the pKa of 4-CP (9.3), pKa of phenol (9.9) and pH point zero charge of the m-RMF (pH_{zpc} = 7.8). At pH 7.8, 9.3 and 9.9, the phenol, 4-CP and the nitrogen species on m-RMF surface are neutral, which favors the hydrophobic and/or π-π stacking interactions between m-RMF and unionized adsorbates which in turn led to maximum removal at said pH values. However, when the solution pH is higher than pKa, the phenol and 4-CP dissociate gradually and are present in solution as phenolate ions ($C_6H_5O^-$) and ($C_6H_5ClO^-$) respectively. Hence, in the very alkaline solution (pH > pKa), there was a reduction in the adsorption capacity of the adsorbent towards both phenols due to the electrostatic repulsion between the negatively charged phenolate ions and negatively charged surface of m-RMF ($pH > pH_{zpc}$).

At solution lower than the pH_{zpc} of m-RMF which is 7.8, the surface of m-RMF was positively charged ($pH < pH_{zpc}$) while majority of adsorbate molecules were neutral and not ionized (pH < pKa). Hence, the removal observed in the acidic medium might be due to the formation of hydrogen bond by H-acceptors (NH_2 and CH_3) on the surface of m-RMF and H-donors of the phenolic compounds.

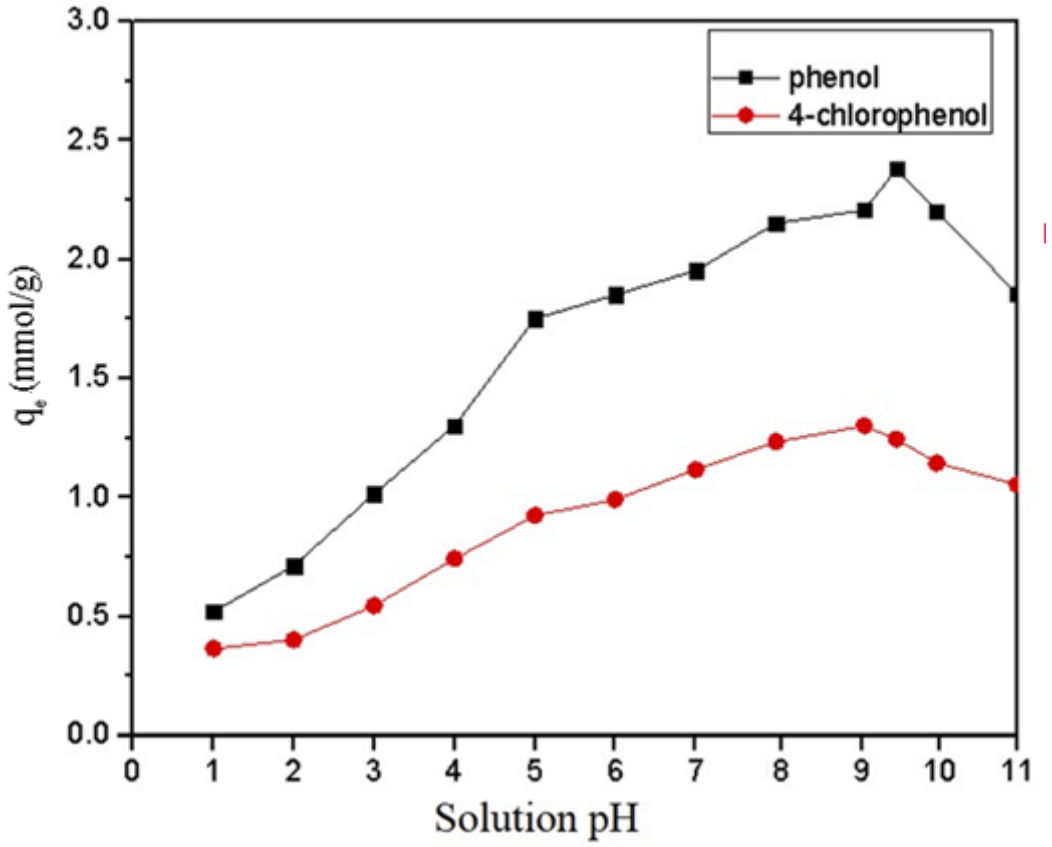

Figure 17. Effect of initial pH on phenol and 4-CP adsorption. Experimental condition: adsorbate concentration: 10 mmol/L, adsorption time: 45 min, m-RMF dosage: 0.1 g/L, T: 298 K

4.2.9 Effect of solution pH on R-g-Ch

The effect of solution pH on the performance of the R-g-Ch beads and pH_{zpc} of R-g-Ch is shown in Figure 18. Apparently, the adsorption process was also pH dependent and high removal capacity was achieved in alkaline condition. The uptake capacity increased steadily in the pH range of 1-9 but decreased when the solution pH exceeded pH 9 due to the electrostatic repulsions between the anionic adsorbates and the negative surface of the R-g-Ch. The higher adsorption performance in alkaline condition is possibly related to the pKa values of 4-CP (9.3), phenol (9.9), and the pH_{zpc} of the R-g-Ch (pH_{zpc} = 8.3).

At pH 8.3, 9.3 and 9.9, the R-g-Ch, 4-CP, and phenol respectively become neutral, which favors the hydrophobic interactions between R-g-Ch and unionized adsorbates. In the acidic region, the surface of R-g-Ch beads was positively charged and the hydrophobic interaction was weakened however the formation of the H- bonding between the R-g-Ch beads and the phenolic compounds attributed to the adsorption observed in this pH range. Similar observations were reported in the case of m-RMF.

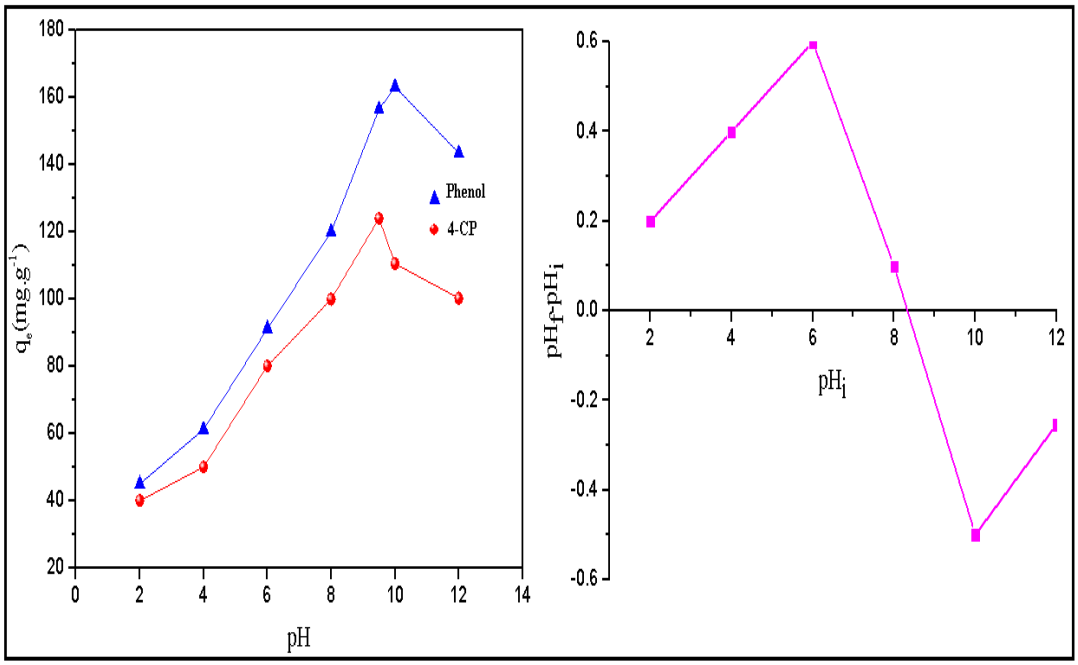

Figure 18: Effect of initial pH value on adsorption capacity of R-g-Ch

4.2.10 Effects of initial concentration and solution temperature on R-g-Ch

The phenolic compound solutions with different concentrations (1–200 mg/L) were used to investigate the effect of initial concentration of phenol and 4–CP adsorption in the presence of 0.5 g R-g-Ch at 25°C. Figure 19a shows that the equilibrium uptake capacity increased with an increase in the adsorbate initial concentration. Particularly, the removal capacity increased from 41.4 mg/g to 180.9 mg/g for phenol and from 12.06 to 95.5 mg/g for 4–CP when the adsorbate concentrations were increased from

1 to 100 mg/L. The increase in the adsorbate concentration increased the probability of collisions between the phenol or 4–CP molecules and R-g-Ch beads which in turn resulted in enhanced interaction between the adsorbates and the available active binding sites on the R-g-Ch [196]. Also, an increase in mass gradient acts as a driving force to overcome the mass transfer resistances of adsorbate molecules from the bulk solution to the R-g-Ch surface [192].

Fig. 19b shows that after increasing the temperature of the adsorption system, the removal capacity decreases. The results obviously revealed that the removal capacity decreased from ~181 mg/g at 25°C to 125 mg/g at 45°C. The decrease in the removal capacity with increasing temperature is attributed to damage of active binding sites and weakening of binding forces between the R-g-Ch and adsorbate molecules [196].

Also, with increasing solution temperature, the solubility of phenolics in water increased and led to a decrease in the removal capacity. The observed trend revealed that the adsorption of the phenolics herein by the R-g-Ch beads is an exothermic process [209].

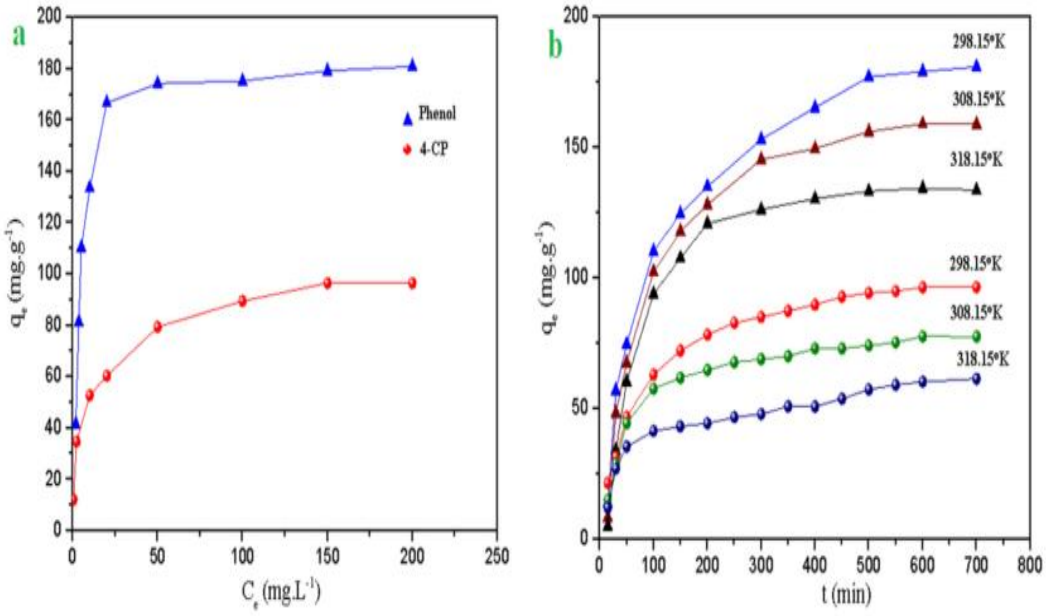

Figure 19: Effect of (a) initial concentration (b) solution temperature on the removal capacity of R-g-Ch for phenol and 4–CP

4.3 Adsorption isotherms

4.3.1 Adsorption Isotherm study of m-RMF

As depicted in Figure 20(a-d), the adsorption amounts of phenol and 4-CP on m-RMF as a function of equilibrium concentrations was well represented linearly, suggesting that the adsorption of the phenolic compounds herein occurred at specific homogeneous sites and can be satisfactorily fitted by the Langmuir isotherm model. As shown in Table 1, the R^2 values of Freundlich isotherm equations in the range of 0.958-0.961 were comparatively low when compared to the Langmuir model (0.9952 and 0.9954), thus cannot describe the experimental data well. Also, since the Freundlich constant n was greater than 1, it revealed that the surface of m-RMF is homogeneous and the adsorption process is favorable [198, 210,211].

Table 4: Isotherms parameters for adsorption of phenol and 4-chlorophenol on m-RMF

	Langmuir			Freundlich		
Adsorbate	q_m (mmol/g)	K_L L/mmol)	R^2	K_F mmol/g	n (L/mmol)	R^2
Phenol	2.49	1.18	0.9952	1.03	2.59	0.9546
4-cp	1.50	0.7 4	0.9954	0.57	2.09	0.9634

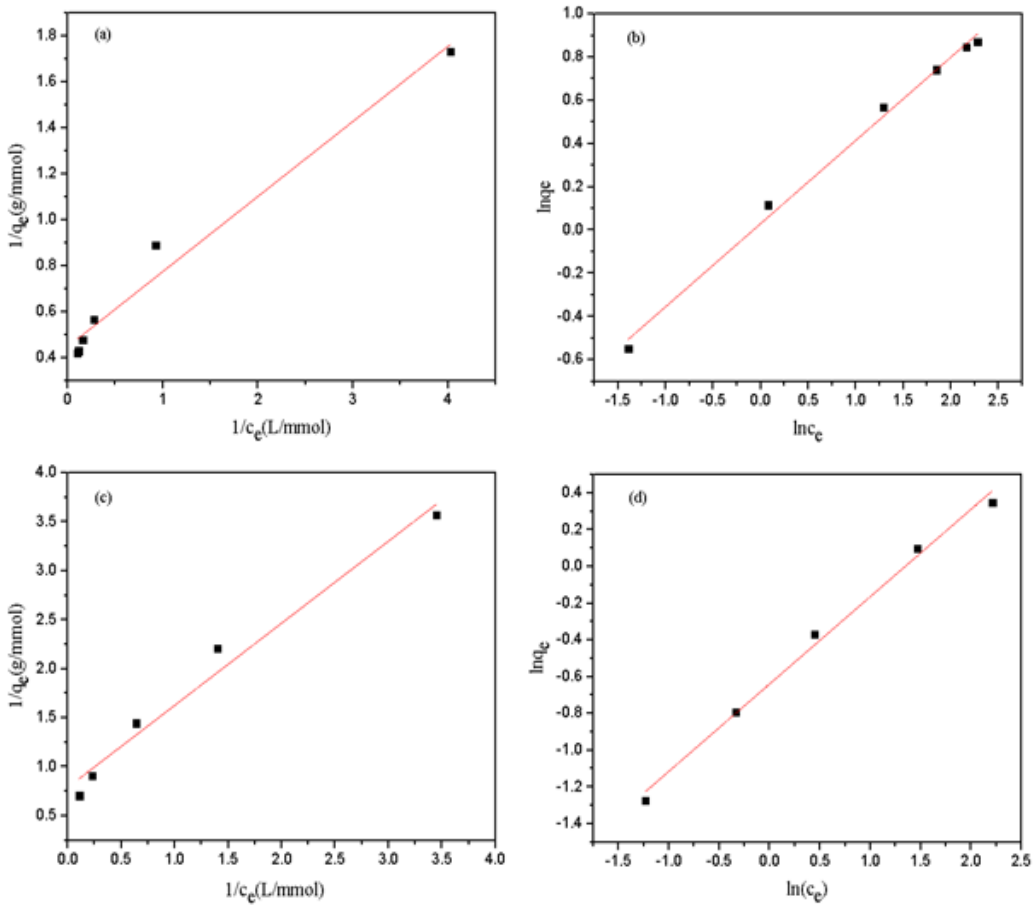

Figure 20: Langmuir and Freundlich isotherm of phenol (a and b), 4-cholorophenol (c and d) on m-RMF

4.3.2 Proposed adsorption mechanism of phenolic compound on m-RMF

It is commonly known that hydrophobicity, hydrophilicity, and polarity of adsorbate and adsorbent can play a key role in adsorption. According to Lewis acid-base theory, the melamine and benzene ring of adsorbate can be considered as Lewis base, while phenolic compound ring viewed as Lewis acid. There are two types of interaction between solute and adsorbate: 1) hydrophobic and van der Waals interaction between phenyl ring on surface adsorbate and phenol 2) the amine group of melamine could provide proton acceptor for hydrogen bonding from hydroxyl group of phenolic compounds therefore, making it possible that the phenolic compound adsorbed onto the surface melamine and phenyl groups through hydrogen bonding and π-π interaction respectively (Scheme 2). Among the phenolic compound, 4-CP has more hydrophobic characteristic than phenol due to possessing of the electronegative group (Cl) on the benzene ring, therefore it has the lower adsorption against phenol.

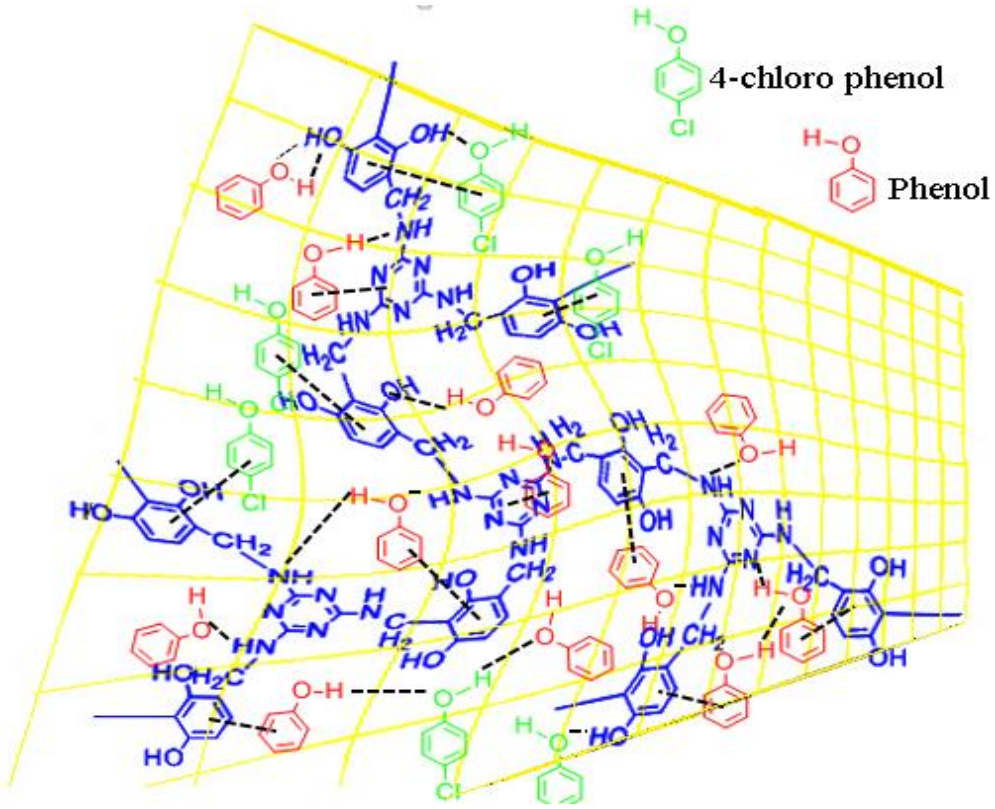

Scheme 6: mechanism of adsorption of phenolic compound on m-RMF

4.3.3 Adsorption Isotherm study of R-g-Ch

Linear plots of the Langmuir and Freundlich isotherm for the removal of both phenols in depicted in Figure 21 while the obtained constants and R^2 values for each model are described in Table 2. The results from the table shows that Langmuir model is the best fitting model to the experimental data rather than Freundlich isotherm model with respect to the correlation co-efficient obtained (0.99). R_L and 1/n values calculated shows that the adsorption process is favorable for all concentrations.

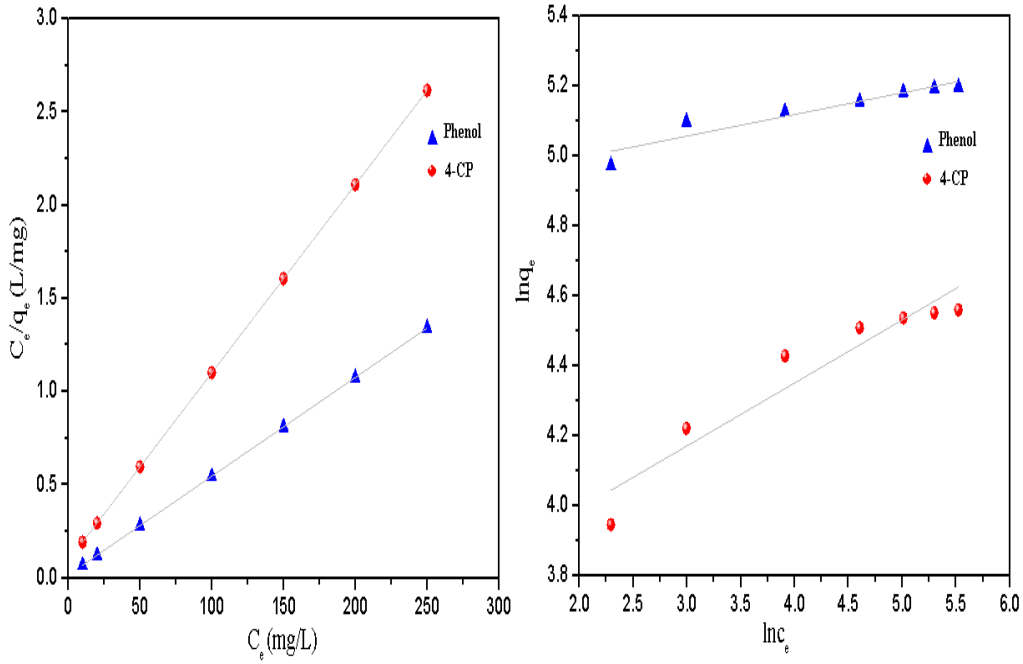

Figure 21: The Langmiur (a) and Freundlich (b) adsorption isotherms on R-g-Ch.

Table 5: Langmuir and Freundlich parameters for adsorption of phenol and 4-CPon R-g-Ch

Adsorbate	Langmuir isotherm				Freundlich isotherm		
	q_m (mg/g)	K_L (L/mg)	R_L	R^2	K_F ((mg/g)(L/mg)$^{1/n}$)	1/n	R^2
Phenol	188.6	0.32	0.02	0.99	58	0.25	0.96
4-CP	99	0.1	0.06	0.99	37.3	0.18	0.90

4.4 Adsorption Kinetics

4.4.1 Kinetic studies on m-RMF

The controlling mechanism of adsorption of the phenolic compounds on m-RMF were studied using pseudo- first -order and pseudo-second-order kinetic models. In the pseudo-first-order, Lagrange equation was used to evaluate adsorption of adsorbate from solution. The corresponding kinetic parameters of pseudo-first and second order

were calculated from related Figures (22 and 23) and listed in table4.3. The results from the table indicates that the correlation co-efficient of pseudo-first-order is lower than pseudo-second-order, therefore pseudo-second-order kinetic model of phenolic compounds was the best fit for the adsorption process.

Table 6: Kinetic model parameters for the adsorption of phenol and 4–CP by the m-RMF beads

Kinetic model	parameters	phenol	4-CP
Pseudo-first order	Q_{tecal} (mg/g)	2.34	1.56
	K_1(1/min)	0.003	0.048
	R^2	0.970	0.980
	ARE	3.25	2.95
Pseudo-second order	$Q_{e,cal}$ (mg/g)	2.30	1.53
	K_1(1/min)	0.096	0.070
	R^2	0.999	0.999
	ARE	2.31	3.12

Initial concentration: 10mmol/L ; dosage of adsorbate: 0.1g

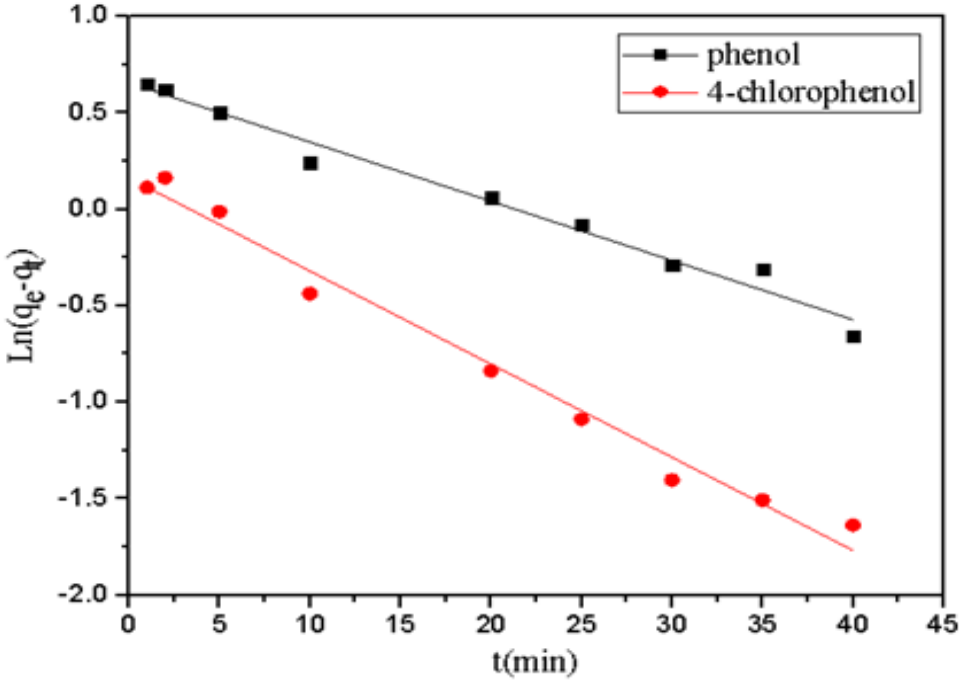

Figure 22: The adsorption model of pseudo-first-order on m-RMF

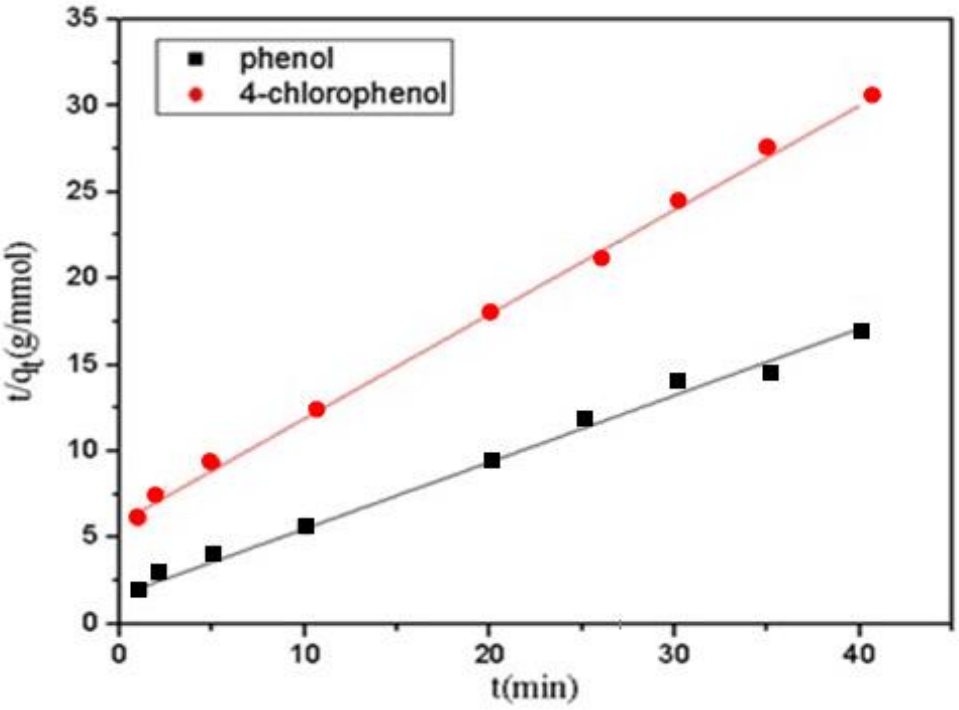

Figure 23: The adsorption model of pseudo-second-order on m-RMF

4.4.2 Kinetic studies on R-g-Ch

Similarly, three well known kinetic models were studied to better understand the possible mechanism of phenol and 4-CP removal by R-g-Ch and to determine the adsorption efficiency. They include; pseudo first, pseudo second order and intra-particle diffusion model. Figure 24 presents the fitting plots for pseudo first and second order kinetic models and Table 4.4 shows the kinetic parameters obtained from the modeling. The results obtained from table 4.4 shows the pseudo-second-order modeling are in agreement with the sorption of the phenolic compound by R-g-Ch. Concerning the adsorption models, the kinetics are better described by the pseudo-second-order n model. For the pseudo-second-order model, the pseudo rate constant K_2 is equal to 0.03, 0.02 $gmg^{-1}s^{-1}$ and the maximum amount predicted by the model is 180.9, 95.5mg g^{-1} for phenol and 4-CP, respectively. In the case of the pseudo-second-order n model, a higher value of R^2 gives a better fitting (see Figure 24 and Table 4.4), and produces predicted maximum amounts that are close to the experimental one. The maximum amount obtained from the Langmuir model for phenol and 4-CP are 188.6 and 99 mg/g.

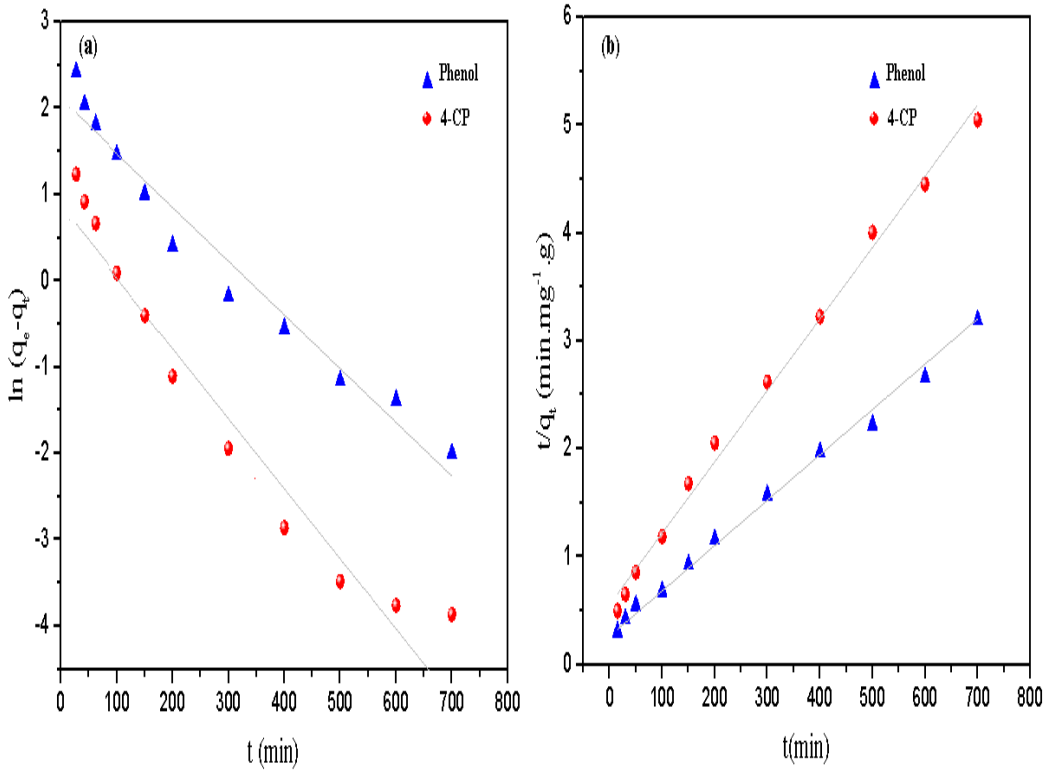

Figure 24: Pseudo-first order (a) and pseudo-second order (b) adsorption kinetics on R-g-Ch

Table 7: Kinetic model parameters for the adsorption of phenol and 4–CP by the R-g-Ch beads

Kinetic model	parameters	Phenol	4-CP
Pseudo-first order	$Q_{t,cal}$ (mg/g)	161.3	128.2
	K_1(1/min)	0.002	0.006
	R^2	0.960	0.880
	ARE	6.46	5.98
Pseudo-second order	$Q_{t,cal}$ (mg/g)	204.1	96.2
	K_2(1/min)	0.030	0.020
	R^2	0.999	0.999
	ARE	2.31	3.12
Intraparticle diffusion	C	14.37	9.29
	K_{id}(mg/min$^{0.5}$)	0.134	0.115
	R^2	0.979	0.993
	ARE	2.24	3.56

q_e = 180.9 mg/g for phenol and 95.5 mg/g for 4–CP. Initial concentration: 80 mg/L; R-g-Ch beads dosage: 0.5 g.

4.5 Thermodynamic adsorption on R-g-Ch

Adsorption experiments of both phenol and 4-CP were carried out at three different temperatures. The Van't Hoff plot of *In* K_D as a function of the inverse of time is shown in figure 25 and yields a straight line. As presented in Table 3, the negative values of ΔG° and ΔS° suggest that the adsorption process is spontaneous and a decrease in the degree of disorder at the solid/solution interface was obtained during the adsorption process, respectively. Also, the negative values of the enthalpy change ΔH^o confirms the exothermic nature of the adsorption, supported by the decreasing adsorption of the phenolic compounds with an increase in temperature [212].

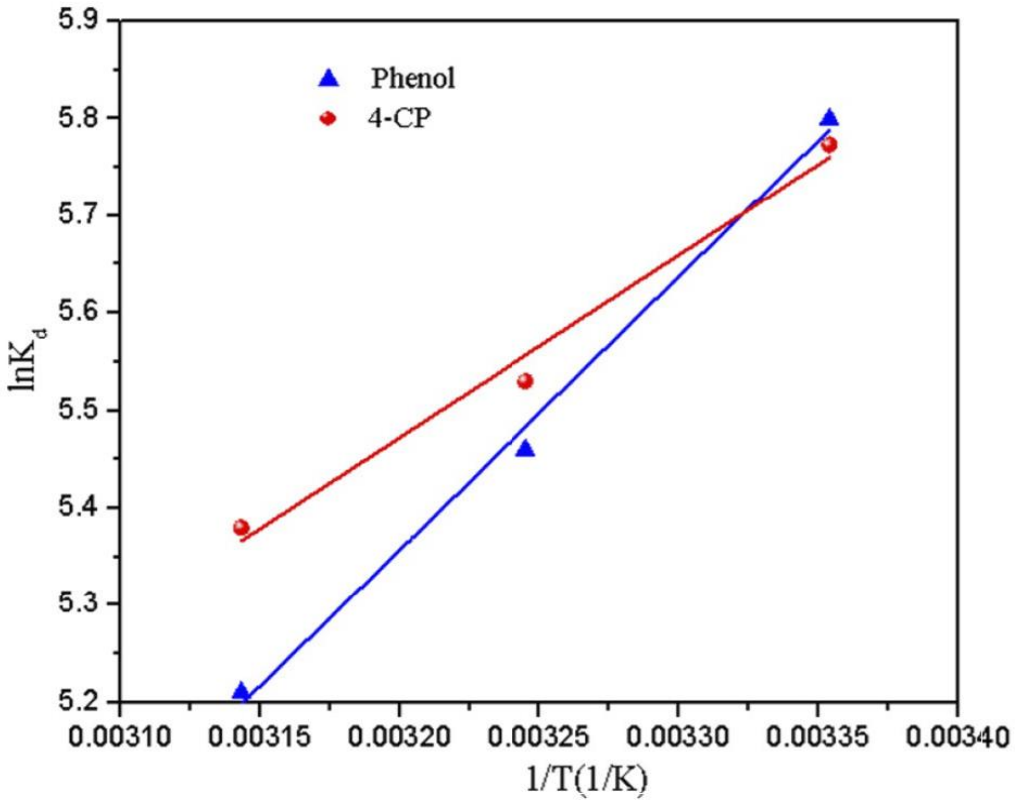

Figure 25: Van't Hoff plot for the adsorption of phenol and 4-CP onto R-g-Ch

Table 8: Thermodynamic data for adsorption of phenolic compounds on R-g-Ch

	R^2	ΔH^o (kJ mol^{-1})	ΔS^o (J mol^{-1} K^{-1})	ΔG^o(kJ mol^{-1})		
				298.15 ^oK	308.15^oK	318.15^oK
Phenol	0.99	-23.29	-29.9	-14.37	-14.08	-13.93
4-CP	0.97	-15.54	-4.2	-14.29	-14.24	-14.22

Chapter 5

CONCLUSION

Our present study investigated the potential of a mesoporous magnetic resin (m-RMF) and porous magnetic resin-chitosan beads (R-g-Ch) for the removal of phenols (4-CP and phenol) from simulated waste water under laboratory conditions using batch adsorption technique. The effect of various operational parameters such as; contact time, initial adsorbent dosage, adsorbate concentration, temperature and pH were examined to determine optimum conditions for the removal of both phenolic compounds from water and the adsorption capacity of both adsorbents. The physical structure, surface morphology and textural characterization of both adsorbents were also carried out. Experimental results obtained were then used to study the sorption mechanism, kinetics and thermodynamics of both adsorbents during phenol and 4-CP removal.

The analysis of all experimental results shows that the removal efficiency of both phenol and 4-CP was influenced by various factors including pH, time, dosage and initial adsorbate concentration. The maximum adsorption capacity for 0.1 g (optimum dosage) of m-RMF in both adsorbate solutions (10 mmol/L) at 298 k for 45 min was 2.49 and 1.5 mmol/mg for phenol and 4-chlorophenol respectively while that of 0.3 g (optimum dosage) of R-g-Ch in 25 ml, 80 mg/L (phenol or 4-CP solution) for 700 min was 180.9 and 95.5mg. It was also observed that an increase in the initial concentration of the adsorbates resulted in an increase in the amount of adsorbates adsorbed onto

both R-g-Ch and m-RMF. 4–CP showed a lower adsorption capacity than phenol on both adsorbents due to the presence of the electronegative chlorine group on its benzene ring. Interestingly, both adsorbents could be easily separated from the reaction medium due to their magnetic properties exhibited.

A comparison of the kinetic data (Table 4.6) of both m-RMF and R-g-Ch confirms that both adsorption processes are controlled by the pseudo-second-order equation since the correlation coefficients obtained was higher than that of other models studied as well. According to the parameters determined from the intra-particle diffusion model of R-g-Ch, the phenol and 4-CP adsorption mechanism is a complex process and intra-particle diffusion was not the only rate controlling step.

Table 9: Kinetic model parameters for the adsorption of phenol and 4–CP by the m-RMF and R-g-Ch beads

		parameters	phenol	4-CP
Pseudo-first order	R-g-Ch	$Q_{t,cal}$ (mg/g)	161.3	128.2
		K_1(1/min)	0.002	0.006
		R^2	0.960	0.880
		ARE	6.46	5.98
	m-RMF	$Q_{t,cal}$ (mg/g)	180.6	149.76
		K_1(1/min)	0.03	0.048
		R^2	0.97	0.98
		ARE	—	—
Pseudo-second order	R-g-Ch	$Q_{t,cal}$ (mg/g)	204.1	96.2
		K_1(1/min)	0.030	0.020
		R^2	0.999	0.999
		ARE	2.31	3.12
	m-RMF	$Q_{t,cal}$ (mg/g)	216.45	196.68
		K_1(1/min)	0.096	0.07
		R^2	0.99	0.99
		ARE	—	—
Intra-particle diffusion	R-g-Ch	C	14.37	9.29
		K_1(mg/min$^{0.5}$)	0.134	0.115
		R^2	0.979	0.993
		ARE	2.24	3.56
	m-RMF	$Q_{t,cal}$ (mg/g)	—	—
		K_1(1/min)	—	—
		R^2	—	—
		ARE	—	—

To further predict the adsorption mechanism of both adsorbents, two isotherm model were applied and the results shows that Langmuir model has better fitting than the Freundlich model as seen in Table 4.7 (i.e. higher correlation coefficients values R^2 and maximum adsorption is high in Langmuir model). According to the R_L values which are less than 1, we understand that the phenol uptake occurred on the homogeneous surface of both adsorbents by monolayer adsorption without interaction between adsorbate molecules. This was determined to be the favorable mechanism for the adsorption process. The lower values of R_L obtained for phenols when compared to 4-CP shows that interaction between phenols is stronger than that of 4-CP.

Table 10: Isotherm model parameters for the adsorption of phenol and 4–CP by the m-RMF and R-g-Ch beads.

		parameters	phenol	4-CP
Langmuir	R-g-Ch	q_m (mg/g)	188.6	99
		K_L(1/min)	0.320	0.100
		R^2	0.999	0.999
		ARE	2.66	1.33
	m-RMF	q_m (mg/g)	243.33	192
		K_L(1/min)	1.18	0.79
		R^2	0.995	0.995
		ARE	—	—
Freundlich	R-g-Ch	K_f (mg/g(L/mg)$^{1/n}$)	58.3	37.3
		1/n	0.25	0.18
		R^2	0.960	0.900
		ARE	5.45	3.12
	m-RMF	K_f (mg/g(L/mg)$^{1/n}$)	1.03	0.57
		1/n	0.47	0.32
		R^2	0.958	0.960
		ARE	—	—

Finally, the effects of temperature on the removal of both phenolic compounds were explored. Negative Gibbs free energy (ΔG°) and enthalpy change (ΔH°) confirm the adsorption process to be spontaneous and exothermic in nature while negative entropy change (ΔS°) shows the decreased disorderliness at the solid - solution interface. Furthermore, it should be noted that an increase in temperature reduces the kinetics of the phenol uptake.

In conclusion, based on the all results obtained and analyzed within the framework of this thesis study, it appears that both adsorbents (m-RMF and R-g-Ch) can serve as a good adsorbent for eradication of both phenolic compounds from waste water.

REFERENCES

[1] Goel, P. (2006). *Water pollution: causes, effects and control: New Age International*.

[2] Cornwell, D. A., & Davis, M. L. (2012). *Introduction to environmental engineering*: Mcgraw-hill Education-Europe.

[3] Agarwal, S. K. (2009). *Heavy metal pollution* (Vol. 4): APH publishing.

[4] Nitrate/Nitrate. Online on the internet from http:// www.epa.gov/ogwdw/dwh/t-ioc/nitrate.html.

[5] Haas, C. N. (1995). *Hazardous and industrial waste treatment*.

[6] Revenga, C., & Mock, G. (2000). *Dirty water: Pollution problems persist. Pilot Analysis of Global Ecosystems: Freshwater Systems*.

[7] Corcoran, E., Nellemann, E., Baker, R., Bos, D., & Osborn, H. Savelli (eds). (2010) *Sick Water? The central role of waste-water management in sustainable development*. A Rapid Response Assessment: United Nations Environment Programme, un-habitat, griD-Arendal.

[8] Dönmez, G. Ç., Aksu, Z., Öztürk, A., & Kutsal, T. (1999). A comparative study on heavy metal biosorption characteristics of some algae. *Process biochemistry*, 34(9), 885-892.

[9] Pérez-Rama, M., Alonso, J. A., López, C. H., & Vaamonde, E. T. (2002). Cadmium removal by living cells of the marine microalga Tetraselmis suecica. *Bioresource Technology*, 84(3), 265-270.

[10] Mahvi, A. (2008). Application of agricultural fibers in pollution removal from aqueous solution. *International Journal of Environmental Science & Technology*, 5(2), 275-285.

[11] Balasubramanian, A., & Venkatesan, S. (2012). Removal of phenolic compounds from aqueous solutions by emulsion liquid membrane containing ionic liquid [BMIM]+[PF6]− in tributyl phosphate. *Desalination*, 289, 27-34.

[12] Radovic, L. R., Moreno-Castilla, C., & Rivera-Utrilla, J. (2001). Carbon materials as adsorbents in aqueous solutions. *Chemistry and physics of carbon*, 227-406.

[13] Busca, G., Berardinelli, S., Resini, C., & Arrighi, L. (2008). Technologies for the removal of phenol from fluid streams: a short review of recent developments. *Journal of Hazardous Materials*, 160(2-3), 265-288.

[14] Ahmaruzzaman, M. (2008). Adsorption of phenolic compounds on low-cost adsorbents: a review. *Advances in colloid and interface science*, 143(1-2), 48-67.

[15] Singh, D., & Srivastava, B. (2002). Removal of phenol pollutants from aqueous solutions using various adsorbents. *Journal of science industrial Research*. 61, 208-218.

[16] Namasivayam, C., & Kavitha, D. (2003). Adsorptive removal of 2-chlorophenol by low-cost coir pith carbon. *Journal of hazardous materials*, 98(1-3), 257-274.

[17] Nazari, K., Esmaeili, N., Mahmoudi, A., Rahimi, H., & Moosavi-Movahedi, A. (2007). Peroxidative phenol removal from aqueous solutions using activated peroxidase biocatalyst. *Enzyme and Microbial Technology*, 41(3), 226-233.

[18] ulkarni, S. J., & Kaware, J. P. (2013). Review on research for removal of phenol from wastewater. *International Journal of Scientific and Research Publications*, 3(4), 1-5.

[19] Radeke, K., Lohse, U., Struve, K., Weib, E., & Schröder, H. (1993). Comparing adsorption of phenol from aqueous solution onto SiO2 faujasite, activated carbons, and polymeric resins. *Zeolites*, 13(1), 69-70.

[20] Jung, M.-W., Ahn, K.-H., Lee, Y., Kim, K.-P., Rhee, J.-S., Park, J. T., & Paeng, K.-J. (2001). Adsorption characteristics of phenol and chlorophenols on granular activated carbons (GAC). *Microchemical journal*, 70(2), 123-131.

[21] Muraleedharan, T., Iyengar, L., & Venkobachar, C. (1991). Biosorption: an attractive alternative for metal removal and recovery. *Current Science*, 61(6), 379-385.

[22] Jagwani, D., & Joshi, P. (2014). Deportation of toxic phenol from aqueous system by wheat husk. *International Journal of Plant, Animal and Environmental Sciences*, 4(2), 58-64.

[23] Mustafa, A. I., Alam, M. S., Amin, M. N., Bahadur, N. M., & Habib, A. (2008). Phenol removal from aqueous system by jute stick. *Pakistan Journal of Analytical & Environmental Chemistry*, 9(2), 4.

[24] Kilic, M., Apaydin-Varol, E., & Pütün, A. E. (2011). Adsorptive removal of phenol from aqueous solutions on activated carbon prepared from tobacco residues: equilibrium, kinetics and thermodynamics. *Journal of Hazardous Materials*, 189(1-2), 397-403.

[25] Goud, V. V., Mohanty, K., Rao, M., & Jayakumar, N. (2005). Phenol removal from aqueous solutions by tamarind nutshell activated carbon: batch and column studies. Chemical Engineering & Technology: Industrial Chemistry-Plant Equipment-Process Engineering-*Biotechnology*, 28(7), 814-821.

[26] Streat, M., Patrick, J., & Perez, M. C. (1995). Sorption of phenol and para-chlorophenol from water using conventional and novel activated carbons. *Water Research*, 29(2), 467-472.

[27] Mattson, J. A., Mark Jr, H. B., Malbin, M. D., Weber Jr, W. J., & Crittenden, J. C. (1969). Surface chemistry of active carbon: specific adsorption of phenols. *Journal of Colloid and Interface Science*, 31(1), 116-130.

[28] Coughlin, R. W., Ezra, F. S., & Tan, R. N. (1968). Influence of chemisorbed oxygen in adsorption onto carbon from aqueous solution. *Journal of colloid and interface Science*, 28(3-4), 386-396.

[29] Daifullah, A., & Girgis, B. (1998). Removal of some substituted phenols by activated carbon obtained from agricultural waste. *Water research*, 32(4), 1169-1177.

[30] Singh, B., Misra, N., & Rawat, N. (1994). Sorption characteristics of phenols on fly ash and impregnated fly ash. *Indian Journal of Environmental Health*, 36(1), 1-7.

[31] Dentel, S., Bottero, J., Khatib, K., Demougeot, H., Duguet, J., & Anselme, C. (1995). Sorption of tannic acid, phenol, and 2, 4, 5-trichlorophenol on organoclays. *Water Research*, 29(5), 1273-1280.

[32] Singh, D., & Mishra, A. (1993). Removal of organic pollutants by the use of iron (III) hydroxide-loaded marble. *Separation science and technology*, 28(10), 1923-1931.

[33] Singh, D., & Mishra, A. (1990). Removal of phenolic compounds from water by using chemically treated saw dust. *Indian journal of environmental health*, 32(4), 345-351.

[34] Singh, D., & Darbari, A. (1987). Ligand exchange chromatography separations of some phenolic compounds on zinc silicate in Fe (III) form. *Journal of liquid chromatography*, 10(14), 3235-3248.

[35] Viraraghavan, T., & de Maria Alfaro, F. (1998). Adsorption of phenol from wastewater by peat, fly ash and bentonite. *Journal of Hazardous Materials*, 57(1-3), 59-70.

[36] Mahadeva Swamy, M., Mall, I., Prasad, B., & Mishra, I. (1998). Sorption characteristics of O-cresol on bagasse fly ash and activated carbon. *Indian journal of environmental health*, 40(1), 67-78.

[37] Singh, D., & Srivastava, B. (2000). Removal of some phenols by activated carbon developed from used tea leaves. *Journal of Industrial Pollution Control*, 16(1), 19-30.

[38] Mahesh, S., Chitranshi, U., & Deepak, D. (1998). Adsorption kinetics of dihydric phenol: Catechol on activated carbon. *Indian Journal of Environmental Health*, 40(2), 169-176.

[39] Palanichamy, M., Joseph, B., & Chandran, S. (1994). Adsorption kinetics of phenol on controlled burnt wood charcoal system. *Indian J. Environ. Prot*, 14, 591-594.

[40] Singh, D., Srivastava, B., & Yadav, P. (2002). Iron oxide coated sand as an adsorbent for separation and removal of phenols. *Indian Journal of Chemical Technology*. 9, 285-289.

[41] Mahesh, S., Rama, B., Praveena Kumari, H., & Usha Lakshmi, K. (1999). Adsorption kinetics of dihydric phenol-hydroquinone on activated carbon. *Indian Journal of Environmental Health*, 41(4), 317-325.

[42] Mckay, G., Bino, M., & Altamemi, A. (1985). The adsorption of various pollutants from aqueous solutions on to activated carbon. *Water Research*, 19(4), 491-495.

[43] McGuire, M. J., & Suffet, I. H. (1981*). Activated carbon adsorption of organics from the aqueous phase: Ann Arbor Science.*

[44] Himmelstein, K., Fox, R., & Winter, T. (1973). In-place regeneration of activated carbon. Chem. *Engng Prog*, 69(11), 65-69.

[45] Praveen, K., & Bhatia, S. (1994). Separation of phenol and para-cresol from dilute aqueous waste streams. *Indian J. Environ. Protec*, 14, 490-496.

[46] Crook, E. H., McDonnell, R. P., & McNulty, J. T. (1975). Removal and recovery of phenols from industrial waste effluents with Amberlite XAD polymeric adsorbents. *Industrial & Engineering Chemistry Product Research and Development*, 14(2), 113-118.

[47] Devarajulu, T., Rambabu, K., Krishnaiah, A., & Viswanath, D. (1999). Adsorption of phenol, p-nitrophenol and their binary mixtures from aqueous solutions on amberlite synthetic resin XAD-2. *Indian Journal of Environmental Protection*, 19(11), 838-841.

.

[48] Kennedy, D. C. (1973). Macroreticular polymeric adsorbents. *Industrial & Engineering Chemistry Product Research and Development*, 12(1), 56-61.

[49] Deshmukh, S., & Pangarkar, V. (1984). Recovery of organic chemicals from effluents by adsorption over polymeric adsorbents. *Indian Chem. Eng*, 26(3), 35-38.

[50] Goto, M., Hayashi, N., & Goto, S. (1986). Adsorption and desorption of phenol on anion-exchange resin and activated carbon. *Environmental science & technology*, 20(5), 463-467.

[51] Reddy, K. A., Anand, P., & Dasare, B. (1989). Sorption of phenolic compounds by porous polymeric adsorbents. *Indian J Environ Health*, 31, 197-206.

[52] Farrier, D. S., Hines, A. L., & Wang, S. W. (1979). Adsorption of phenol and benzoic acid from dilute aqueous solution onto a macroreticular resin. *Journal of Colloid and Interface Science*, 69(2), 233-237.

[53] Reddy, K., Anand, P., & Dasare, B. (1989). Sorption of phenolic compounds on porous weakly basic anion exchangers based on acrylic matrix. *Indian Journal of Environmental Health*, 31(4), 297-303.

[54] Anderson, R., & Hansen, R. (1955). Phenol sorption on ion exchange resins. *Industrial & Engineering Chemistry*, 47(1), 71-75.

[55] Srivastava, S. K., Jain, C. K., Oberoi, C. K., & Sharma, A. K. (1982). Kinetics and mechanism of ion exchange sorption of some detergents on zinc ferrocyanide. *Canadian Journal of Chemistry*, 60(13), 1681-1686.

[56] Huang, T.C., & Cho, L.T. A. (1988). The adsorption of phenol on anion exchange resins in the presence of p-nitrophenol. *Chemical Engineering Communications*, 74(1), 169-177.

[57] Goto, S., Goto, M., & Uchiyama, S. (1984). Adsorption equilibria of phenol on anion exchange resins in aqueous solution. *Journal of chemical engineering of Japan*, 17(2), 204-205.

[58] Lee, K.-C., & Ku, Y. (1996). Removal of chlorophenols from aqueous solution by anion-exchange resins. *Separation science and technology*, 31(18), 2557-2577.

[59] Huang, T. C. (1988). Batch adsorption of p-nitrophenol and p-chlorophenol on anion exchange resin. *Journal of chemical engineering of Japan*, 21(5), 498-503.

[60] Kawabata, N., Higuchi, I., & Yoshida, J.-i. (1981). Removal and recovery of organic pollutants from the aquatic environment. VII. Adsorption of phenol and carboxylic acids on crosslinked poly (4-vinylpyridine). *Bulletin of the Chemical Society of Japan*, 54(11), 3253-3258.

[61] Abdul Kader, K., Uthayavani, J., & Subramanian, E. (1998). Sorption and removal of phenols form water using crosslinked polyvinylpyrrolidone. *Indian Journal of Environmental Protection*, 18(3), 181-184.

[62] Petronio, B., Lagana, A., & Russo, M. V. (1981). Some applications of ligand-exchange—I. Recovery of phenolic compounds from water. *Talanta*, 28(4), 215-220.

[63] Lundell, G. E. F., Hoffman, J. L (1958) *OutlinesofMethod of Chemical Analysis*, Wiley, New York, 1958, p. 117.

[64] Rawat, J., Mujtaba, S., & Thind, P. (1976). Chromatographic separation and identification of phenols on paper impregnated with stannic molybdate. Fresenius' *Journal of Analytical Chemistry*, 279(5), 368-368.

[65] Nabi, S., Farooqui, W., & Rahman, N. (1985). A semicrystalline inorganic ion-exchanger for thin-layer chromatographic separation of phenolic compounds. *Chromatographia*, 20(2), 109-111.

[66] Siouffi, A., Righezza, M., & Guiochon, G. (1986). Separation of aromatic compounds by liquid chromatography on diol-bonded phase columns. *Journal of Chromatography A*, 368, 189-202.

[67] Lepri, L., Desideri, P., Landini, M., & Tanturli, G. (1975). Chromatographic behaviour of phenols on thin layers of cation and anion exchangers: II. Dowex 50-X4 and Rexyn 102. *Journal of Chromatography* A, 109(2), 365-376.

[68] Singh, D., & Mehrotra, P. (1988). Iron (III) Diethanolamine as a Ne Adsorbent for Chromatographic Separations of Phenols. *Journal of liquid chromatography*, 11(7), 1415-1432.

[69] Rawat, J., & Iqbal, M. (1983). Ligand exchange separation of phenols on alumina in Fe (III) form. *Chromatographia*, 17(12), 701-704.

[70] Liu, J., & Huang, C. (1992). Adsorption of some substituted phenols onto hydrous ZnS (s). *Journal of colloid and interface science*, 153(1), 167-176.

[71] Alata, T., & Tarannum, H. (1999). Removal of O-Nitrophenol and O-Aminophenol by Nickel, Cobalt and Cadmium ferrocyanides. *Journal of Industrial Pollution Control*, 15, 57-64.

[72] Singh, D., & Mishra, A. (1992). Chromatographic separation of some phenols by new adsorbent. *Journal of liquid chromatography*, 15(2), 369-380.

[73] Singh, D., & Srivastava, B. (2000). Iron (III) morpholine gel-a new adsorbent selective for pyrocatechol and pyrogallol. *Chemia Analityczna*, 45(5), 725-734.

[74] Zogorski, J., & Faust, S. (1978). Equilibria of adsorption of phenols by granular activated carbon. *In Chemistry of Wastewater Technology*. Edited by, 143-160.

[75] Martin, R. J. (1980). Activated carbon product selection for water and wastewater treatment. *Industrial & Engineering Chemistry Product Research and Development*, 19(3), 435-441.

[76] Bhatia, S., Kalam, A., Joglekar, H., & Joshi, J. (1990). Effective diffusivity of phenol in activated carbon. *Chemical engineering communications*, 98(1), 139-154.

[77] Caturla, F., Martin-Martinez, J., Molina-Sabio, M., Rodriguez-Reinoso, F., & Torregrosa, R. (1988). Adsorption of substituted phenols on activated carbon. *Journal of colloid and interface science*, 124(2), 528-534.

[78] Aytek n, Ç. (1991). Application of the Polanvi Adsorption Potential Theory to Adsorption Phenolic Compounds from Water Solution onto Activated Carbon. *Spectroscopy letters*, 24(5), 653-664.

[79] Samaras, P., Diamadopoulos, E., & Sakellaropoulos, G. P. (1995). Relationship between the activated carbon surface area and adsorption model coefficients for removal of phenol from water. *Water Quality Research Journal*, 30(2), 325-338.

[80] Asakawa, T., & Ogino, K. (1984). Adsorption of phenol on surface-modified carbon black from its aqueous solution. *Journal of colloid and interface Science*, 102(2), 348-355.

[81] Gudyno TV & Belousora M Ya.1993. *Deposited Doc VI NIT*, 1929-84, I 2pp (Russ) Avail viniti.

[82] Orshansky, F., & Narkis, N. (1997). Characteristics of organics removal by PACT simultaneous adsorption and biodegradation. *Water Research*, 31(3), 391-398.

[83] Kilduff, J. E., & King, C. J. (1997). Effect of carbon adsorbent surface properties on the uptake and solvent regeneration of phenol. *Industrial & engineering chemistry research*, 36(5), 1603-1613.

[84] Furuya, E., Chang, H., Miura, Y., Yokomura, H., Tajima, S., Yamashita, S., & Noll, K. (1996). Intraparticle mass transport mechanism in activated carbon adsorption of phenols. *Journal of Environmental Engineering*, 122(10), 909-916.

[85] Mostafa, M., Samra, S., & Youssef, A. (1989). Removal of organic pollutants from aqueous-solution. 1. Adsorption of phenols by activated carbons. *Indian journal of chemistry section a-inorganic bio-inorganic physical theoretical & analytical chemistry*, 28(11), 946-948.

[86] Yen, C.-y., & Singer, P. C. (1984). Competitive adsorption of phenols on activated carbon. *Journal of Environmental Engineering*, 110(5), 976-989.

[87] Khan, A., Al-Bahri, T., & Al-Haddad, A. (1997). Adsorption of phenol based organic pollutants on activated carbon from multi-component dilute aqueous solutions. *Water Research*, 31(8), 2102-2112.

[88] Talinli, I., & El-mabrouk, F. A. (1994). Enhanced removal of phenol and m-cresol in PAC additional activated sludge system. *Environmental technology*, 15(12), 1121-1134.

[89] Mazet, M., Farkhani, B., & Baudu, M. (1994). Influence of heat or chemical treatment of activated carbon onto the adsorption of organic compounds. *Water Research*, 28(7), 1609-1617.

[90] Vidic, R., Suidan, M., Sorial, G., & Brenner, R. (1994). Effect of molecular oxygen on adsorptive capacity and extraction efficiency of granulated activated

carbon for three ortho-substituted phenols. *Journal of hazardous materials*, 38(3), 373-388.

[91] Julien, F., Baudu, M., & Mazet, M. (1994). Effects of the modification of the activated carbon physico-chemical characteristics onto the organic compounds adsorption. Aqua- Journal of Water Supply. *Research and Technology*, 43(6), 278-286.

[92] El-Shahawi, M. (1993). Preconcentration and separation of some organic water pollutants with polyurethane foam and activated carbon. *Chromatographia*, 36(1), 318-322.

[93] Rivera-Utrilla, J., Utrera-Hidalgo, E., Ferro-Garcia, M., & Moreno-Castilla, C. (1991). Comparison of activated carbons prepared from agricultural raw materials and Spanish lignites when removing chlorophenols from aqueous solutions. *Carbon*, 29(4-5), 613-619.

[94] Srivastava, S., & Tyagi, R. (1995). Competitive adsorption of substituted phenols by activated carbon developed from the fertilizer waste slurry. *Water Research*, 29(2), 483-488.

[95] Rayalu, S., & Shrivastava, A. (1993). Adsorption of phenol on new adsorbent activated carbon cloth. *Indian J. Environ. Prot*, 13(6), 407-514.

[96] Abuzaid, N. S., & Nakhla, G. F. (1994). Dissolved oxygen effects on equilibrium and kinetics of phenolics adsorption by activated carbon. *Environmental science & technology*, 28(2), 216-221.

[97] Mcmanus C M A. Werthman H P, Westendorf R J. *Proc Thirtyninth Ind Was1e Conf*. (1985) pp 719.

[98] Kim, B. R., Chian, E. S., Cross, W. H., & Cheng, S.-S. (1986). Adsorption, desorption, and bioregeneration in an anaerobic, granular activated carbon reactor for the removal of phenol. *Journal Water Pollution Control Federation*, 35-40.

[99] Tanada, M., Miyoshi, T., Nakamura, T., & Tanada, S. (1990). Adsorption removal of cresol by granular activated carbon for medical waste water treatment. *Bulletin of environmental contamination and toxicology*, 45(2), 170-176.

[100] Sorial, G. A., Suidan, M. T., Vidic, R. D., & Maloney, S. W. (1993). Competitive adsorption of phenols on GAC. I: adsorption equilibrium. *Journal of Environmental Engineering*, 119(6), 1026-1043.

[101] Wang, R. C., Kuo, C. C., & Shyu, C. C. (1997). Adsorption of phenols onto granular activated carbon in a liquid–solid fluidized bed. *Journal of Chemical Technology & Biotechnology*: International Research in Process, Environmental AND Clean Technology, 68(2), 187-194.

[102] Ha, S., & Vinitnantharat, S. (2000). Competitive removal of phenol and 2, 4-dichlorophenol in biological activated carbon system. *Environmental technology*, 21(4), 387-396.

[103] Asakawa, T., & Ogino, K. (1984). Adsorption of phenol on surface-modified carbon black from its aqueous solution. *Journal of colloid and interface Science*, 102(2), 348-355.

[104] Mahajan, O. P., Moreno-Castilla, C., & Walker Jr, P. (1980). Surface-treated activated carbon for removal of phenol from water. *Separation science and technology*, 15(10), 1733-1752.

[105] Lin, S., & Cheng, M. (2000). Phenol and chlorophenol removal from aqueous solution by organobentonites. *Environmental technology*, 21(4), 475-482.

[106] Boyd, S. A., Shaobai, S., Lee, J.-F., & Mortland, M. M. (1988). Pentachlorophenol sorption by organo-clays. *Clays Clay Miner*, 36(2), 125-130.

[107] Dentel, S. K., Jamrah, A. I., & Sparks, D. L. (1998). Sorption and cosorption of 1, 2, 4-trichlorobenzene and tannic acid by organo-clays. *Water Research*, 32(12), 3689-3697.

[108] Dentel, S. K., Jamrah, A. I., & Sparks, D. L. (1998). Sorption and cosorption of 1, 2, 4-trichlorobenzene and tannic acid by organo-clays. *Water Research*, 32(12), 3689-3697.

[109] Scott, H., Wolf, D., & Lavy, T. (1982). Apparent Adsorption and Microbial Degradation of Phenol by Soil 1. *Journal of Environmental Quality*, 11(1), 107-112.

[110] Hudson-Baruth, B., & Seitz, M. (1986). Adsorption of select phenol derivatives by dolomite. Environmental Pollution Series B, *Chemical and Physical*, 11(1), 15-28.

[111] Isaacson, P. J., & Frink, C. R. (1984). Nonreversible sorption of phenolic compounds by sediment fractions: the role of sediment organic matter. *Environmental science & technology*, 18(1), 43-48.

[112] Laquer, F. C., & Manahan, S. E. (1987). Solution factors affecting the adsorption of phenol onto a siltstone. *Chemosphere*, 16(7), 1431-1445.

[113] Schellenberg, K., Leuenberger, C., & Schwarzenbach, R. P. (1984). Sorption of chlorinated phenols by natural sediments and aquifer materials. *Environmental science & technology*, 18(9), 652-657.

[114] Rny A S & Ram B. (1990). Adsorption characteristics of some phenol and phenolic effluents on sodium and TEBA- rnonunorillonitc. *Indian J Environ Protect*. 10, 816.

[115] Zhu, L., Chen, B., & Shen, X. (2000). Sorption of phenol, p-nitrophenol, and aniline to dual-cation organobentonites from water. *Environmental Science & Technology*, 34(3), 468-475.

[116] Zhu L, Li Y, Zhang J. (1997). Sorption of organobentonites to some organic pollutants in water. *Environmental science & technolog.* 31(5):1407-10.

[117] Mudhukumar, A., & Anirudhan, T. (1994). Phenol exchange characteristics of sediment samples from coconut husk retting zones. *Ind. J. Env. Prot*, 14, 772.

[118] Srivastava, S., Gupta, V., Johri, N., & Mohan, D. (1995). Removal of 2, 4, 6-trinitrophenol using bagasse fly ash-A sugar industry waste material.

[119] Rozich, A., Gaudy Jr, A. F., & D'Adamo, P. (1983). Predictive model for treatment of phenolic wastes by activated sludge. *Water Research*, 17(10), 1453-1466.

[120] Stapleton, M. G., Sparks, D. L., & Dentel, S. K. (1994). Sorption of pentachlorophenol to HDTMA-clay as a function of ionic strength and pH. *Environmental science & technology*, 28(13), 2330-2335.

[121] Mahadevaswamy, M., Mall, I., Prasad, B., & Mishra, I. (1997). *Removal of phenol by adsorption on coal fly ash and activated carbon*.

[122] Satapathy, B., & Rao, D. R. (1984). Adsorption Efficiency of High-Carbon Fly-Ash. *Research and Industry*, 29(3), 188-190.

[123] Shei MS & Cheny S L. *Proc Fonythird Ind Water*. 1988.

[124] Sarkar A, Singh B K & Ram B. Role of carbonaceous matter in fly ash in removing pollutants from coke oven and synthetic phenol plant effluents. *Indian J Environ Protect*, 10(1990)367.

[125] Banarjce K. Hong P Y. Scheremissoff P N, Shlih M S & Chanj S L. (1988). *Int Conj Physicochem Biol Detox Hazard Waste*.1, 249.

[126] Haribabu, E., Upadhya, Y., & Upadhyay, S. (1993). Removal of phenols from effluents by fly ash. *International journal of environmental studies*, 43(2-3), 169-176.

[127] Kumar, S., Upadhyay, S., & Upadhya, Y. (1987). Removal of phenols by adsorption on fly ash. *Journal of Chemical Technology & Biotechnology*, 37(4), 281-290.

[128] Deepak, D., Shankaranarayana, K., & Chandramauli, V. (1988). Removal of phenol from waste water by adsorption on fly ash and soil. *Asian Environment*, 10(2), 37-42.

[129] Khanna, P., & Malhotra, S. (1977). Kinetics and mechanism of phenol adsorption on fly ash. *Indian J. Environ. Health*, 19(3), 224-237.

[130] Aksu, Z., & Yener, J. (1999). The usage of dried activated sludge and fly ash wastes in phenol biosorption/adsorption: comparison with granular activated carbon. *Journal of Environmental Science & Health Part A*, 34(9), 1777-1796.

[131] Xing, B., McGill, W. B., Dudas, M. J., Maham, Y., & Hepler, L. (1994). Sorption of phenol by selected biopolymers: isotherms, energetics, and polarity. *Environmental science & technology*, 28(3), 466-473.

[132] Severtson, S. J., & Banerjee, S. (1996). Sorption of chlorophenols to wood pulp. *Environmental science & technology*, 30(6), 1961-1969.

[133] El-Shahawi, M., Farag, A., & Mostafa, M. (1994). Preconcentration and separation of phenols from water by polyurethane foams. *Separation science and technology*, 29(2), 289-299.

[134] Srivastava, S., Pant, N., & Pal, N. (1987). Studies on the efficiency of a local fertilizer waste as a low cost adsorbent. *Water research*, 21(11), 1389-1394.

[135] Zogorski, J. S., & Faust, S. D. (1977). Operational parameters for optimum removal of phenolic compounds from polluted waters by columns of activated carbon. Paper presented at the Water. *AICHE Symposium Series American Institute of Chemical Engineers*.

[136] Wu, F. C., Tseng, R. L., & Juang, R. S. (1999). Preparation of activated carbons from bamboo and their adsorption abilities for dyes and phenol. *Journal of Environmental Science & Health Part A*, 34(9), 1753-1775.

[137] Fytianos, K., Voudrias, E., & Kokkalis, E. (2000). Sorption–desorption behaviour of 2, 4-dichlorophenol by marine sediments. *Chemosphere*, 40(1), 3-6.

[138] Daughney, C. J., & Fein, J. B. (1998). Sorption of 2, 4, 6-trichlorophenol by Bacillus subtilis. *Environmental science & technology*, 32(6), 749-752.

[139] Ngah, W. W., Teong, L., & Hanafiah, M. (2011). Adsorption of dyes and heavy metal ions by chitosan composites: A review. *Carbohydrate polymers*, 83(4), 1446-1456.

[140] Kumar, A. S. K., Kumar, C. U., Rajesh, V., & Rajesh, N. (2014). Microwave assisted preparation of n-butylacrylate grafted chitosan and its application for Cr (VI) adsorption. *International journal of biological macromolecules*, 66, 135-143.

[141] George Z. K, Dimitrios N. Bikiaris. (2015). Review Recent Modifications of Chitosan for Adsorption Applications: A Critical and Systematic Review. *Mar. Drugs*, 13, 312-337.

[142] Perpétuo, G. J., & Janczak, J. (2008). Supramolecular architectures in crystals of melamine and aromatic carboxylic acids. *Journal of Molecular Structure*, 891(1), 429-436.

[143] Liu, Y. T., Deng, J., Xiao, X. L., Ding, L., Yuan, Y. L., Li, H., . . . Wang, L. L. (2011). Electrochemical sensor based on a poly (para-aminobenzoic acid) film modified glassy carbon electrode for the determination of melamine in milk. *Electrochimica Acta*, 56(12), 4595-4602.

[144] Song, L., Zhao, X., Fu, J., Wang, X., Sheng, Y., & Liu, X. (2012). DFT investigation of Ni (II) adsorption onto MA-DTPA/PVDF chelating membrane in the presence of coexistent cations and organic acids. *Journal of hazardous materials*, 199, 433-439.

[145] Seoighe, C., Naumann, J., & Shvets, I. (1999). Studies of surface structures on single crystalline magnetite (100). *Surface science*, 440(1-2), 116-124.

[146] dovorany, J. R.; Alexander, S. F. US *Patent* 2007/0224409 A1, 2007.

[147] Jaouen, L., Renault, A., & Deverge, M. (2008). Elastic and damping characterizations of acoustical porous materials: Available experimental methods and applications to a melamine foam. *Applied acoustics*, 69(12), 1129-1140.

[148] Kosaka, Y.; Hattori, G.; hattori, G. US *Patent*, 2002/0163105 A1, 2001.

[149] Tomita, B., & Ono, H. (1979). Melamine–formaldehyde resins: Constitutional characterization by fourier transform 13C-NMR spectroscopy. Journal of Polymer Science: *Polymer Chemistry Edition*, 17(10), 3205-3215.

[150] Bal, A., Acar, I., & Güçlü, G. (2012). A novel type nanocomposite coating based on alkyd-melamine formaldehyde resin containing modified silica: Preparation and film properties. *Journal of Applied Polymer Science*, 125(S1), E85-E92.

[151] Weiser, J., Reuther, W., Fikentscher, R., Fath, W., Berbner, H., Zettler, H. D., & Voelker, H. (1994). *Modified melamine-formaldehyde resins*, Google Patents.

[152] Imashiro, Y.; Hasegawa, S.; Okutani, T. US *Patent* 5, 436, 278, 1995.

[153] Spencer, F. R.; Spencer, F. R. US *Patent* 3,093,600, 1963.

[154] Absi-Halabi, M., Lahalih, S., & Al-Khaled, T. (1987). Water-soluble sulfonated amino-formaldehyde resins. I. Melamine resins, synthesis. *Journal of applied polymer science*, 33(8), 2975-2984.

[155] Lee, J., & Yee, A. (2001). Inorganic particle toughening II: toughening mechanisms of glass bead filled epoxies. *Polymer*, 42(2), 589-597.

[156] Liu, Z., Wang, H., Lu, Q., Du, G., Peng, L., Du, Y., Yao, K. (2004). Synthesis and characterization of ultrafine well-dispersed magnetic nanoparticles. *Journal of Magnetism and Magnetic Materials*, 283(2-3), 258-262.

[157] Zhang, D., Zhang, X., Ni, X., Song, J., & Zheng, H. (2007). Fabrication and characterization of Fe3O4 octahedrons via an EDTA-assisted route. Crystal Growth & Design, 7(10), 2117-2119.

[158] Sun, S., & Zeng, H. (2002). Size-controlled synthesis of magnetite nanoparticles. *Journal of the American Chemical Society*, 124(28), 8204-8205.

[159] Wang, M., Wang, N., Tang, H., Cao, M., She, Y., & Zhu, L. (2012). Surface modification of nano-Fe 3 O 4 with EDTA and its use in H 2 O 2 activation for removing organic pollutants. *Catalysis Science & Technology*, 2(1), 187-194.

[160] Che, R. C., Peng, L. M., Duan, X. F., Chen, Q., & Liang, X. (2004). Microwave absorption enhancement and complex permittivity and permeability of Fe encapsulated within carbon nanotubes. *Advanced Materials*, 16(5), 401-405.

[161] Zhuo, R., Feng, H., Chen, J., Yan, D., Feng, J., Li, H., Yan, P. (2008). Multistep synthesis, growth mechanism, optical, and microwave absorption properties of ZnO dendritic nanostructures. *The Journal of Physical Chemistry C*, 112(31), 11767-11775.

[162] Ajayan, P. M., & Tour, J. M. (2007). Materials science: nanotube composites. *Nature*, 447(7148), 1066.

[163] Zhou, L., Li, G., An, T., & Li, Y. (2010). Synthesis and characterization of novel magnetic Fe 3 O 4/polyurethane foam composite applied to the carrier of immobilized microorganisms for wastewater treatment. *Research on chemical intermediates*, 36(3), 277-288.

[164] Salgueiriño-Maceira, V., & Correa-Duarte, M. A. (2007). Increasing the complexity of magnetic core/shell structured nanocomposites for biological applications. *Advanced Materials*, 19(23), 4131-4144.

[165] Bekhite, M. M., Figulla, H.-R., Sauer, H., & Wartenberg, M. (2013). Static magnetic fields increase cardiomyocyte differentiation of Flk-1+ cells derived from mouse embryonic stem cells via Ca2+ influx and ROS production. *International journal of cardiology*, 167(3), 798-808.

[166] Filipič, J., Kraigher, B., Tepuš, B., Kokol, V., & Mandic-Mulec, I. (2012). Effects of low-density static magnetic fields on the growth and activities of wastewater bacteria Escherichia coli and Pseudomonas putida. *Bioresource technology*, 120, 225-232.

[167] Yan, D.-X., Ren, P.-G., Pang, H., Fu, Q., Yang, M.-B., & Li, Z.-M. (2012). Efficient electromagnetic interference shielding of lightweight graphene/polystyrene composite. *Journal of Materials Chemistry*, 22(36), 18772-18774.

[168] Zhang, J., Li, L., Chen, G., & Wee, P. (2009). Influence of iron content on thermal stability of magnetic polyurethane foams. *Polymer Degradation and Stability*, 94(2), 246-252.

[169] Wiman, S., Wurmb, V., Litterst, F., Dieckmann, R., & Becker, K. (1998). The temperature-dependent cation distribution in magnetite. *Journal of Physics and chemistry of Solids*, 59(3), 321-330.

[170] Liu, J., Qiao, S. Z., Liu, H., Chen, J., Orpe, A., Zhao, D., & Lu, G. Q. (2011). Extension of the Stöber method to the preparation of monodisperse resorcinol–

formaldehyde resin polymer and carbon spheres. *Angewandte Chemie*, 123(26), 6069-6073.

[171] Dwivedi, C., Kumar, A., Juby, K. A., Kumar, M., Wattal, P. K., & Bajaj, P. N. (2012). Preparation and evaluation of alginate-assisted spherical resorcinol–formaldehyde resin beads for removal of cesium from alkaline waste. *Chemical engineering journal*, 200, 491-498.

[172] Wu, Y., Li, Y., Xu, J., & Wu, D. (2014). Incorporating fluorescent dyes into monodisperse melamine–formaldehyde resin microspheres via an organic sol–gel process: a pre-polymer doping strategy. *Journal of Materials Chemistry B*, 2(35), 5837-5846.

[173] Zhou, H., Xu, S., Su, H., Wang, M., Qiao, W., Ling, L., & Long, D. (2013). Facile preparation and ultra-microporous structure of melamine–resorcinol–formaldehyde polymeric microspheres. *Chemical communications*, 49(36), 3763-3765.

[174] Fang, G., Lau, H. F., Law, W. S., & Li, S. F. Y. (2012). Systematic optimisation of coupled microwave-assisted extraction-solid phase extraction for the determination of pesticides in infant milk formula via LC–MS/MS. *Food chemistry*, 134(4), 2473-2480.

[175] Lv, Z., Sun, Q., Meng, X., & Xiao, F.-S. (2013). Superhydrophilic mesoporous sulfonated melamine–formaldehyde resin supported palladium nanoparticles as

an efficient catalyst for biofuel upgrade. *Journal of Materials Chemistry A*, 1(30), 8630-8635.

[176] Tokudome, Y., Nakane, K., & Takahashi, M. (2014). Mesostructured carbon film with morphology-induced hydrophilic surface through a dewetting-free coating process. *Carbon*, 77, 1104-1110.

[177] Mitome, T., Iwai, Y., Uchida, Y., Egashira, Y., Matsuura, M., Maekawa, K., & Nishiyama, N. (2014). Synthesis of mesoporous carbons using a triblock copolymer containing sulfonic acid groups and their capacitance property. *Journal of Materials Chemistry A*, 2(26), 10104-10108.

[178] Augusto F, Hantao LW, Mogollón NG, Braga SC. (2013). New materials and trends in sorbents for solid-phase extraction. *TrAC Trends in Analytical Chemistry*. 1; 43:14-23.

[179] Li, B., Cao, H., Shao, J., Qu, M., & Warner, J. H. (2011). Superparamagnetic Fe_3O_4 nanocrystals@ graphene composites for energy storage devices. *Journal of Materials Chemistry*, 21(13), 5069-5075.

[180] Yang, C., Wu, J., & Hou, Y. (2011). Fe_3O_4 nanostructures: synthesis, growth mechanism, properties and applications. *Chemical Communications*, 47(18), 5130-5141.

[181] Hristov, J., & Fachikov, L. (2007). An overview of separation by magnetically stabilized beds: state-of-the-art and potential applications. *China Particuology*, 5(1-2), 11-18.

[182] Fuertes, A. B., & Tartaj, P. (2006). A facile route for the preparation of superparamagnetic porous carbons. *Chemistry of materials*, 18(6), 1675-1679.

[183] Nakahira, A., Nagata, H., Takimura, M., & Fukunishi, K. (2007). Synthesis and evaluation of magnetic active charcoals for removal of environmental endocrine disrupter and heavy metal ion. *Journal of applied physics*, 101(9), 09J114.

[184] Oliveira, L. C., Rios, R. V., Fabris, J. D., Garg, V., Sapag, K., & Lago, R. M. (2002). Activated carbon/iron oxide magnetic composites for the adsorption of contaminants in water. *Carbon*, 40(12), 2177-2183.

[185] Schwickardi, M., Olejnik, S., Salabas, E.-L., Schmidt, W., & Schüth, F. (2006). Scalable synthesis of activated carbon with superparamagnetic properties. *Chemical communications* (38), 3987-3989.

[186] Zhang, G., Qu, J., Liu, H., Cooper, A. T., & Wu, R. (2007). $CuFe_2O_4$/activated carbon composite: a novel magnetic adsorbent for the removal of acid orange II and catalytic regeneration. *Chemosphere*, 68(6), 1058-1066.

[187] Ao, Y., Xu, J., Fu, D., Shen, X., & Yuan, C. (2008). A novel magnetically separable composite photocatalyst: titania-coated magnetic activated carbon. *Separation and Purification Technology*, 61(3), 436-441.

[188] N. Atsushi, S. Nishida, K. Fukunishi. (2006). Synthesis of magnetic activated carbons for removal of environmental endocrine disrupter using magnetic vector. *Journal of the Ceramic Society of Japan*, 114(1325), 135-137.

[189] Hirsh, S., Bilek, M., Nosworthy, N., Kondyurin, A., Dos Remedios, C., & McKenzie, D. (2010). A comparison of covalent immobilization and physical adsorption of a cellulase enzyme mixture. *Langmuir*, 26(17), 14380-14388.

[190] Madihally, S. V., & Matthew, H. W. (1999). Porous chitosan scaffolds for tissue engineering. *Biomaterials*, 20(12), 1133-1142.

[191] Gazi, M., Oladipo, A. A., Ojoro, Z. E., & Gulcan, H. O. (2017). High-performance nanocatalyst for adsorptive and photo-assisted Fenton-like degradation of phenol: modeling using artificial neural networks. *Chemical Engineering Communications*, 204(7), 729-738.

[192] Oladipo, A. A., Abureesh, M. A., & Gazi, M. (2016). Bifunctional composite from spent "Cyprus coffee" for tetracycline removal and phenol degradation: Solar-Fenton process and artificial neural network. *International journal of biological macromolecules*, 90, 89-99.

[193] Oladipo, A. A., & Gazi, M. (2015). Microwaves initiated synthesis of activated carbon-based composite hydrogel for simultaneous removal of copper (II) ions and direct red 80 dye: A multi-component adsorption system. *Journal of the Taiwan Institute of Chemical Engineers*, 47, 125-136.

[194] Kumar, P. S., Vincent, C., Kirthika, K., & Kumar, K. S. (2010). Kinetics and equilibrium studies of Pb2+ in removal from aqueous solutions by use of nano-silversol-coated activated carbon. *Brazilian Journal of Chemical Engineering*, 27(2), 339-346.

[195] Langmuir, I. (1918). The adsorption of gases on plane surfaces of glass, mica and platinum. *Journal of the American Chemical society*, 40(9), 1361-1403.

[196] Oladipo, A. A., Ifebajo, A. O., & Vaziri, R. (2018). *Green adsorbents for removal of antibiotics, pesticides and endocrine disruptors Green Adsorbents for Pollutant Removal*. Springer pp. 327-351.

[197] Principe, I. A., & Fletcher, A. J. (2018). Parametric study of factors affecting melamine-resorcinol-formaldehyde xerogels properties. *Materials Today Chemistry*, 7, 5-14.

[198] Oladipo, A. A., Abureesh, M. A., & Gazi, M. (2016). Bifunctional composite from spent "Cyprus coffee" for tetracycline removal and phenol degradation: Solar-Fenton process and artificial neural network. *International journal of biological macromolecules*, 90, 89-99.

[199] Yusof, N. A., Rahman, S. K. A., Hussein, M. Z., & Ibrahim, N. A. (2013). Preparation and characterization of molecularly imprinted polymer as SPE sorbent for melamine isolation. *Polymers*, 5(4), 1215-1228.

[200] Mulik, S., Sotiriou-Leventis, C., & Leventis, N. (2007). Time-efficient acid-catalyzed synthesis of resorcinol− formaldehyde aerogels. *Chemistry of Materials*, 19(25), 6138-6144.

[201] Brunauer, S., Emmett, P. H., & Teller, E. (1938). Adsorption of gases in multimolecular layers. *Journal of the American chemical society*, 60(2), 309-319.

[202] Joyner, L. G., Barrett, E. P., & Skold, R. (1951). The determination of pore volume and area distributions in porous substances. II. Comparison between nitrogen isotherm and mercury porosimeter methods. *Journal of the American Chemical Society*, 73(7), 3155-3158.

[203] Ullah, S., Bustam, M., Nadeem, M., Naz, M., Tan, W., & Shariff, A. (2014). Synthesis and thermal degradation studies of melamine formaldehyde resins. *The Scientific World Journal*, 2014.

[204] Oladipo, A.A. in Nanotechnology in Environmental Science, ed. By C.M. Hussain, A.K. Mishra, *Wiley- VCH Verlag GmbH & Co. KGaA*, New Jersey, 2018, p. 685.

[205] Oladipo, A.S., Ajayi,O.A., Oladipo,A.A., Azarmi,S.L., Nurudeen,Y., Atta, A.Y., Ogunyemi,S.S., Chim.C.R. (2018). Comparative Modelling and Artificial Neural Network Inspired Prediction of Waste Generation Rates of Hospitality Industry: The Case of North Cyprus. *Sustainability,* 10(9), 2965.

[206] Madannejad, S., Rashidi, A., Sadeghhassani, S., Shemirani, F., & Ghasemy, E. (2018). Removal of 4-chlorophenol from water using different carbon nanostructures: A comparison study. *Journal of Molecular Liquids*, 249, 877-885.

[207] The International Centre for Diffraction Data (ICDD) [Internet].14 February, 2011.

[208] Mohan, D., & Singh, K. P. (2002). Single-and multi-component adsorption of cadmium and zinc using activated carbon derived from bagasse—an agricultural waste. *Water research*, 36(9), 2304-2318.

[209] A.A. Oladipo, in: C.M. Hussain, A.K. Mishra (Eds.), Nanotechnology in EnvironmentalScience, *Wiley-VCH Verlag GmbH & Co. KGaA*, New Jersey 2018, p. 685.

[210] Othman, M. B. H., Ahmad, Z., Osman, H., Omar, M. F., & Akil, H. M. (2015). Thermal degradation behavior of a flame retardant melamine derivative hyperbranched polyimide with different terminal groups. *RSC Advances*, 5(112), 92664-92676.

[211] Kakavandi, B., Kalantary, R. R., Jafari, A. J., Nasseri, S., Ameri, A., Esrafili, A., & Azari, A. (2015). Pb (II) adsorption onto a magnetic composite of activated carbon and superparamagnetic Fe3O4 nanoparticles: experimental and modeling study. *Clean–Soil, Air, Water*, 43(8), 1157-1166.

[212] Jaafari, K., Elmaleh, S., Coma, J., & Benkhouja, K. (2001). Equilibrium and kinetics of nitrate removal by protonated cross-linked chitosan. *Water Sa*, 27(1), 9-14.